HYDROGEOCHEMICAL AND ENVIRONMENTAL ISOTOPE CHARACTERIZATION OF THE CO_2 SPRINGS ALONG THE BONGWANA FAULT, ITS IMPACT ON FRESH WATER RESOURCES AND IMPLICATIONS FOR CARBON CAPTURE AND STORAGE (CCS) IN SOUTH AFRICA

Mzikayise Nkwane

Submitted in fulfilment of the requirements for the degree of
Master of Science in Hydrogeology

Discipline of Geological sciences
School of Agricultural, Earth and Environmental Science
College of Agriculture, Engineering and Science
University of KwaZulu-Natal
Durban
South Africa

March 2018

As the Candidate's Supervisor, I have approved this dissertation for submission.
Signed: ---------- Name: ----------Date: ----------

PREFACE

The research reported in this dissertation was completed by the candidate while based in the Discipline of Geological Sciences, School of Agricultural, Earth and Environmental Sciences within the College of Agriculture, Engineering and Science, University of KwaZulu-Natal, South Africa. The research was financially supported by the South Africa Centre for Carbon Capture and Storage (SACCCS).

The contents of this work have not been submitted in any form to another university and, except where the work of others is acknowledged in the text, the results reported are due to investigations by the candidate.

Declaration – Publications

Details of contributions to publications that form part and/or include research presented in this dissertation are:

Nkwane, M. and Demlie, M. (2017). Characterization of the CO_2 springs associated with the Bongwana Fault: its impact on surface water and groundwater quality and implications on carbon capture and storage (CCS) in South Africa. 15th Biennial conference of the Groundwater Division (GWD2017: Change-Challenge-opportunity). 16-18 October 2017, Stellenbosch, South Africa.

Nkwane, M. (2017). Analysis and modelling of the impacts of CO_2 springs associated with Bongwana fault on fresh groundwater and surface water quality and implications on carbon capture and storage (ccs) in South Africa. 5th Biennial Carbon Capture and Storage Conference 2017. 18-19 October 2017 Coastlands Hotel & Convention Centre Umhlanga, KZN, South Africa.

DECLARATION: PLAGIARISM

I, Mzikayise Nkwane, declare that:

I. The research reported in this dissertation, except where otherwise indicated or acknowledged, is my original work;

II. This dissertation has not been submitted in full or in part for any degree or examination to any other university;

III. This dissertation does not contain other persons' data, pictures, graphs or other information, unless specifically acknowledged as being sourced from other persons;

IV. This dissertation does not contain other persons' writing, unless specifically acknowledged as being sourced from other researchers. Where other written sources have been quoted, then:

   a. Their words have been re-written but the general information attributed to them has been referenced;

   b. Where their exact words have been used, their writing has been placed inside quotation marks, and referenced;

V. Where I have used material for which publications followed, I have indicated in detail my role in the work;

VI. This dissertation is primarily a collection of material, prepared by myself, published as journal articles or presented as a poster and oral presentations at conferences. In some cases, additional material has been included;

VII. This dissertation does not contain text, graphics or tables copied and pasted from the Internet, unless specifically acknowledged, and the source being detailed in the dissertation and in the References sections.

Signed: Mzikayise Nkwane

Date: 05 March 2018

ABSTRACT

Natural CO_2-rich springs at the Bongwana area in Eastern South Africa emanate from three sites along an 80 km long North-South trending Bongwana Fault. The geological unit that outcrops along the extent of the Fault are the Dwyka Group rocks that are made up of mainly tillites and subordinate sandstones, shales and conglomerates. The objectives of this M.Sc. study is to characterize these CO_2-rich springs and assess their impacts on shallow groundwater and surface water chemistry and consequently to understand the implication of a failed CCS facility. Groundwater and surface samples were collected both at CO_2 emission and CO_2-free springs, boreholes and streams around the length of the studied fault zone for the analyses of major ions, trace elements and environmental isotopes. Additionally, specific electrical conductivity (EC), total dissolved solids (TDS), pH, temperature, dissolved oxygen (DO), redox potential (Eh), total alkalinity, CO_3^{2-} and HCO_3^- concentrations were determined onsite.

The results indicate that all the travertine cone springs located near Umtamvuna River are characterized by Na-Ca-Mg-HCO_3 water types, while boreholes from shallow groundwater and river samples show Ca-Na-Mg-HCO_3 types. Stable isotope ($\delta^{18}O$ and δ^2H) composition of the travertine cone springs shows a major negative shift from the meteoric water lines with $\delta^{18}O$ and δ^2H values ranging from -7.78 to -6.52 ‰ and -21.5 to -17.9 ‰, respectively. While, the stable isotopic composition of shallow groundwater reflects local and modern meteoric recharge. These observations indicate that the reservoir and source of recharge for the deep circulating groundwater are different from the shallow groundwater. Based on onsite hydrogeological, hydrogeochemical, and environmental isotope observations, a hydrogeological conceptual model is proposed, which states that the groundwater recharge for deep circulating groundwater is to the west of the Bongwana fault, located at a higher altitude. From these altitudes, groundwater percolates through deep fractures and faults to greater depths. As groundwater percolates through the rock, it interacts with minerals and the initial recharge chemistry and isotopic composition is altered along the groundwater flow paths. At depth, groundwater dissolves carbonate rocks and as a result CO_2 is generated.

The dissolution of CO_2 in groundwater further drives the leaching of the formation minerals along the flow path. Near the surface, CO_2 exsolves and travertine mainly composed of calcite, amorphous silica and iron hydroxides is formed. Geochemical inverse modelling and bivariate correlation among groundwater hydrochemical parameters for travertine springs indicate that the major geochemical processes that are responsible for the observed chemical composition are the dissolution of calcite, dolomite, Pyrite, Goethite, K-feldspars, fluorite, albite and sylvite and the precipitation of calcite, amorphous silica, iron hydroxide, iron carbonates, kaolinite and CO_2 gas. The carbonate minerals are attributed to the dissolution of carbonate rocks at depth. Feldspars are common from the Dwyka Group Diamictites, whereas the plagioclase feldspar (albite) is probably originating from the recharge area outside of the Dwyka group or leached from the granitic and metamorphic fragments contained within the Dwyka tillites. These inverse modelling results are supported by the saturation indices (SI) for calcite and dolomite in these springs which range from 0.74 to 0.82 and from 0.24 to 1.35, respectively indicating oversaturation with respect to these minerals and subsequent precipitation out of the aqueous solution. The precipitation of calcite, amorphous silica and iron carbonates were confirmed by the XRF, XRD and thin section results of the travertine rock samples. Acidic pH conditions (5.5), elevated TDS (5937 ppm), EC (3271 mS/m) and high trace metals concentration were detected in all CO_2 emission sites compared to CO_2 free streams, springs and boreholes. These results clearly show the impacts of CO_2 on groundwater and surface water quality within the vicinity of emission points. Therefore, it appears that natural CO_2 emission along the Bongwana fault have impacted the ambient groundwater and surface water quality at the emission sites rendering it unfit for human consumption due to elevated concentration of dissolved constituents above safe drinking standards. The implication of this to CCS in South Africa is the fact that any unintended CO_2 leakage into fresh groundwater and surface water resources from a failed subsurface storage facility may impact freshwater resources. Thus, strict scientific site selection protocols and properly designed monitoring systems are required to minimise the risk.

Key Words/Phrases: Bongwana Fault, CO_2-rich springs, Carbon capture and storage, Environmental isotopes, Hydrochemistry, Inverse modelling, South Africa.

ACKNOWLEDGMENTS

The author would like to acknowledge the South African Centre for Carbon Capture and Storage (SACCCS) for financing the research and Dr Demlie Molla, my research supervisor, for his contribution in giving guidance, review and comments during planning of the research, data collection during field work and reviewing the research dissertation.

GCS (water and Environmental Consultants) (Pty) Ltd-Durban office is acknowledged for allowing the author to use their facilities during desktop study and the compilation of the research dissertation and also for the time they allowed the author to take off from work and focus on this research. Many thanks to Hendrik Botha, Callie Pickering and Pieter Labuschagne for their comments and suggestions which greatly improved the quality of the dissertation in terms of scientific knowledge and interpretation of data.

CONTENTS **PAGES**

LIST OF FIGURES

LIST OF TABLES

LIST OF APPENDICES

LIST OF ACRONYMS

CCS : Carbon Capture and Storage

DO : Dissolved Oxygen

EC : Electrical Conductivity

GRIP : Groundwater Resource Information Projects

IAP : Ionic Activity Product

KZN : Kwazulu Natal

MAP : Mean Annual Precipitation

MBGL : Meters below Ground Level

Mg/l : Milligrams per litre

ml : Millilitre

mS/m : Millisiemens per Meter

N/A : Not Applicable

ORP : Oxidation Reduction Potential

PCSP : Pilot Carbon dioxide Storage Project

Ppm : Parts Per Million

SACCCS : South African Centre for Carbon Capture and Storage

SANS : South African National Standards

SI : Saturation Index

TALK : Total Alkalinity

TDS : Total Dissolved Solids

TMS : Table Mountain Sandstone

TU : Tritium Units

WRC : Water Research Commission

1. CHAPTER ONE: INTRODUCTION

1. 1 Background to the research

Various comprehensive studies on global climate change have concluded that recent increases in the average global temperature are most likely the effect of the increase in concentration of carbon dioxide (CO_2) and other greenhouse gases in the atmosphere. The increase in CO_2 concentrations in the atmosphere, as a result of anthropogenic activities, has been tagged as a major cause of global climate change. This is because CO_2 is a primary greenhouse gas and the increase in its concentration in the atmosphere has significant impacts on climate change.

Carbon capture and storage in deep geologic formations, which aims at capturing and injecting CO_2 into deep subsurface rock formations for long-term storage, is being explored worldwide as an option to reduce the impact of CO_2 emissions on global climate change and human health (Dafflon, et al., 2012; Benson and Cook, 2005; IPCC, 2007).

In South Africa, the Carbon Capture and Storage (CCS) activities are undertaken by the South African Centre for Carbon Capture and Storage (SACCCS). SACCCS is undertaking pilot studies to investigate the feasibility of capturing and injecting CO_2 in deep saline aquifers in South Africa. Pilot studies are being undertaken in the Zululand basin in KwaZulu-Natal and the Algoa Basin in the Eastern Cape.

The major concern with carbon dioxide sequestration in deep geologic formations is the unintended leakage of CO_2 from the storage reservoir into the fresh groundwater aquifers and the resultant associated impacts on groundwater quality (Yang, 2014). Research shows that the dissolution of CO_2 in groundwater lowers pH and may further mobilise naturally occurring trace metals and ions that are commonly adsorbed on to or contained in sediments (Daflon, 2012; Kharaka, 2009; Smyth, 2008; Benson, 2006; CO_2GeoNet, 2011).

Since CO_2 sequestration is a new concept in South Africa, groundwater and surface water monitoring along the Bongwana fault was considered as an excellent analogue to study the impacts of a failed CO_2 storage site, as natural CO_2 emits at various points along the fault. The two leakage scenarios from a failed CCS facility under consideration are the abrupt leakage through injection well failure or leakage from an abandoned well, and gradual leakage through undetected faults, fractures or wells.

Therefore, this research seeks to characterise groundwater that is associated with the CO_2 springs in terms of its hydrochemical and isotope composition and demonstrate, with field and laboratory evidence, the risks associated with dissolution of carbon dioxide in fresh water resources. The research will form basis for the selection of the most likely geochemical changes that can be monitored around the CO_2 underground storage facility that can indicate the intrusion of CO_2 in groundwater and surface water resources.

1.2 Problem statement

The South African Centre for Carbon Capture and Storage (SACCCS) is investigating the feasibility of undertaking a pilot CO_2 capture and storage study in deep geologic formations in South Africa. The challenge facing the pilot project is the lack of monitoring data related to impacts of CO_2 on fresh water resources if an unforeseen release of CO_2 from an underground storage facility occurs.

The area along the Bongwana fault was suggested by SACCCS as a relevant analogue site to undertake groundwater monitoring and to understand the impacts of CO_2 release on freshwater resources. However, there is insufficient information and data showing the interaction of CO_2 emanating along the Bongwana Fault with fresh water resources.

1.3 Hypothesis

The CO_2 springs associated with the Bongwana fault provides an excellent analogue to study the impacts of CO_2 leakage from a failed underground storage facility into fresh groundwater and surface water resources under the two leakage scenarios, namely; sudden leakage through injection well failure or leakage up an abandoned well, and gradual leakage, through undetected faults, fractures or wells.

1.4 Research questions

In order to prove the above mentioned hypothesis, the following research questions were generated:

- What is the ambient groundwater and surface water quality in the study area without the impacts of CO_2?
- What are the most likely geochemical processes that contribute to the evolution of groundwater and surface water chemistry?
- Can the introduction of CO_2 in groundwater and surface water in the study area affects the ambient water chemistry? And how?
- What are the geological, hydrogeological and hydrochemical characteristics within the study area?
- Are there any other sources of contaminants within the study area that could potentially result in the same impacts as CO_2?

1.5 Research aim and objectives

The aim of this research is to assess the impacts the CO_2 springs have on fresh groundwater and surface water quality in the Bongwana area and to supply a scientific understanding of the risks to fresh water resources associated with the pilot CCS in South Africa as well as to recommend mitigation measures to minimize the risk.

The main objectives of this M.Sc. Research are**:**

- To characterise the CO_2 springs associated with the Bongwana fault.
- To assess their impacts on fresh groundwater and surface water quality by assessing the hydro-geochemical changes in groundwater as a result of the introduction of CO_2 in groundwater and surface water.
- To understand the possible source of the chemical parameters in groundwater and recharge for groundwater for the Bongwana area.
- Comment on the feasibility, potential risks of the CCS activities in the Zululand Basin of South Africa.
- Supply recommendations on the groundwater and surface water monitoring plans for the pilot CCS site in South Africa.

- Comment on the chemical determinants that can be used as indicators of CO_2 leakage from the storage site into the fresh water aquifer.

1.6 **Dissertation structure**

Chapter one: This chapter provides an overview of the research project including statement of the problem and research aims and objectives.

Chapter two: This chapter presents the geographic location of the study area and discusses the climatic, geological and hydrogeological conditions of the study area. The information used in this chapter was gathered through the assessment of the previous geological and hydrogeological reports conducted within the study area as well as geological and hydrogeological maps published for the area.

Chapter three: this literature review chapter discusses the sources of carbon dioxide emissions and its impacts as a greenhouse gas and further discusses the processes that are involved in the capturing, transporting and sequestration of carbon dioxide as an effort to curb its emissions. Furthermore, the chapter discusses the migration of CO_2 gas within the earth's crust and how it affects groundwater and surface water quality. Most of the information used in this chapter is based on papers and reports from previous studies conducted around the world where natural CO_2 sites have been used to understand CO_2 migration within the earth's crust and the impacts on groundwater and surface water associated with the dissolution of CO_2 in water.

Chapter four: this chapter describes the methodology used to in undertaking the research project. It describes a sequence of tasks completed in order to make sure the research was a success. These tasks include the gathering of information on a desktop level, field assessment, laboratory analysis as well as data analysis and interpretation. All the information gathered during each task is used to inform the study.

Chapter five: This chapter presents all the results obtained during the field assessment and laboratory analysis. The information is displayed in the form of tables, graphs and diagrams. The field assessment data include the in-situ water quality parameters, groundwater level measurements in boreholes, field titration, among others. The laboratory data includes hydrochemistry, environmental isotopes, petrography, and geochemical data on travertine composition.

Chapter six: discusses the findings of the study and presents the interpretation based on the results obtained. The information discussed in this chapter is based on the analysis of information collected during the desktop survey, field assessment and laboratory analysis. Based on the overall findings of the study, a conceptual model is proposed that illustrates the origin, occurrence and circulation of the CO_2 rich spring along the Bongwana Fault.

Chapter seven concludes with the main findings of the research, the outcome of which presents technical recommendations for groundwater monitoring requirements related to CCS in deep underground storage facilities. Finally, all references used in the preparation of the dissertation are listed under list of references.

2. CHAPTER 2: DESCRIPTION OF THE STUDY AREA

2.1 Location of the study area

A large part of the study area falls within the boundaries of Umziwabantu Local Municipality of the Ugu District Municipality. The Bongwana fault is located on the border between KwaZulu Natal and the Eastern Cape (Figure 2-1). The fault is approximately 80 km long and runs from west of Port Shepstone in KZN to the south of Bizana in the Eastern Cape. Three sites along the fault, where CO_2 gas issues from the fault gouge, have been identified. These sites are known as Umzimkulwana River, Mbangweni River and Umtamvuna River.

Umzimkulwana River CO_2 emission site: In this site, CO_2 issues from an approximately 20 m wide fault gouge within the beds of Umzimkulwana River. CO_2 samples obtained by Young (1923) and reported in Gevers (1941) indicates CO_2 percentages of 98.3% and 97.6% for 2 samples.

Mbangweni River CO_2 emission site: At this site, CO_2 bubbles from the river beds at the position were the Bongwana fault cuts through the river, however, the bubbles are very small.

Umtamvuna River CO_2 emission site: The CO_2 springs near Umtamvuna River are associated with the deposition of travertine cones with groundwater at low temperatures between 20 and 22 degrees Celsius.

Another site where CO_2 issues from a borehole drilled for water supply occurs parallel to the main fault. This site is believed to be associated with a minor faults parallel to the main fault. This site is referred to as “Farm Lot 4”.

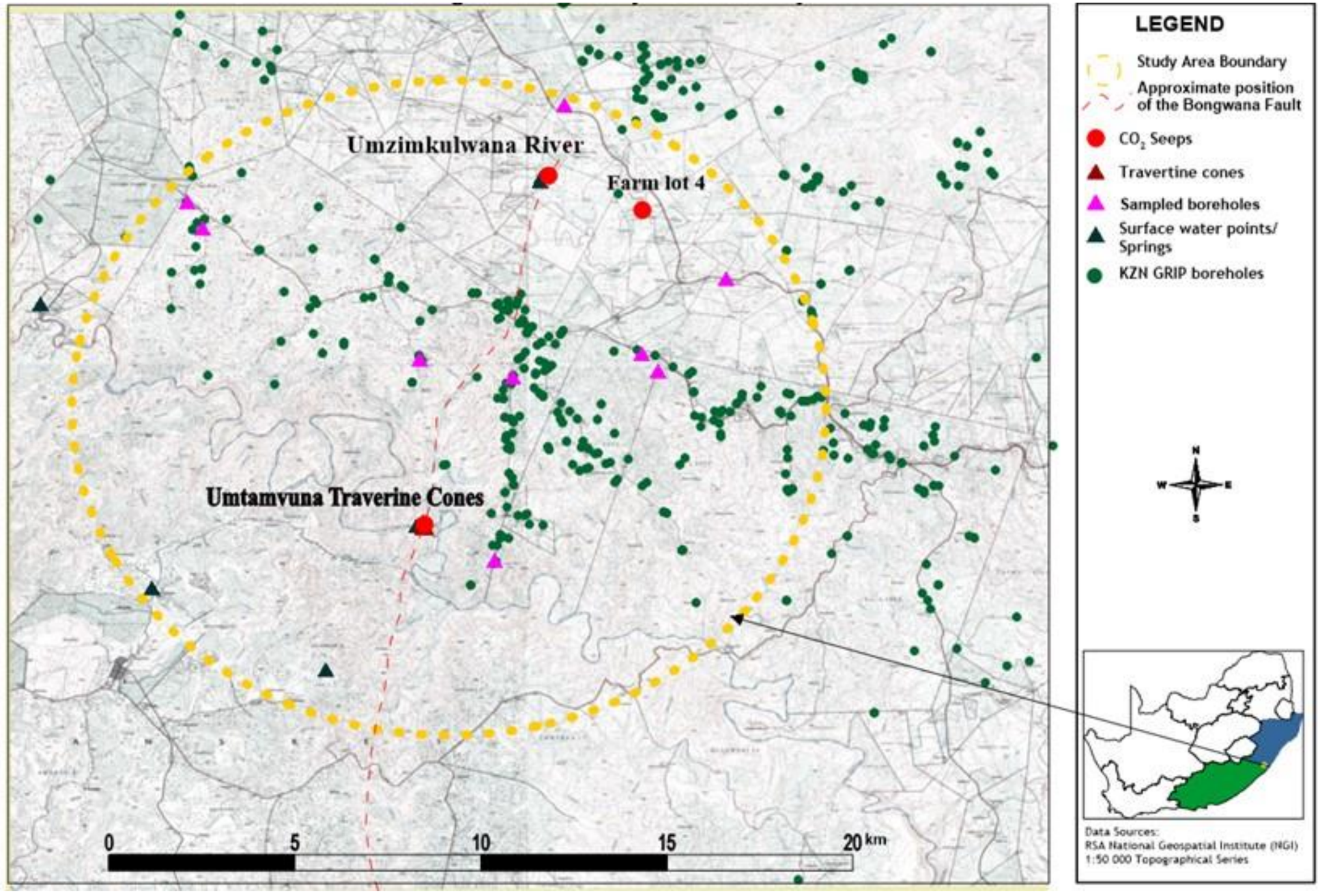

Figure 2-1: Locality map of the study area

2.2 Climate and drainage

The climate of the study area is characterized by warm summers and cool winters. Precipitation in the study area is seasonal, with most rainfall occurring as thunderstorms during the period between October and March. The peak rainfall months are December to January (Figure 2-1). The rate of rainfall increases with increasing altitude, generally from east to west and the mean annual precipitation ranges between 700-1350 mm.

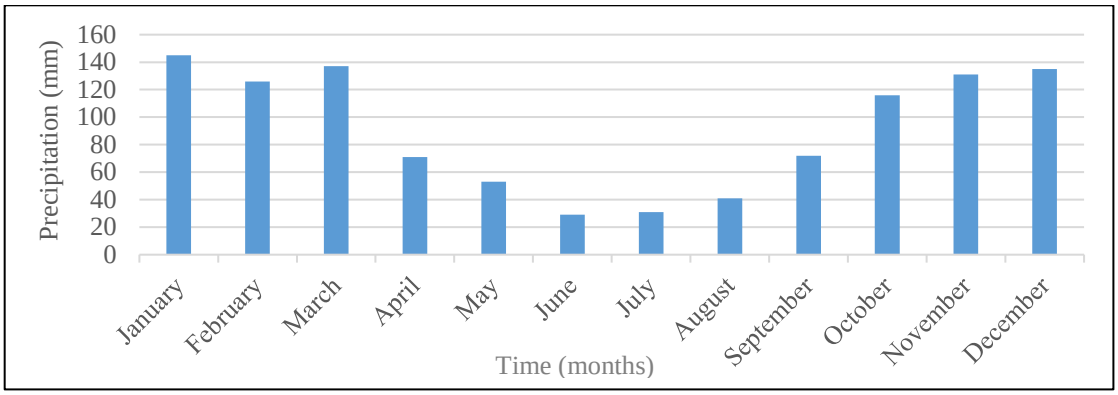

Figure 2-2: Average monthly rainfall for the study area.

The drainage of the study area falls within the Mvoti to uMzimkhulu Water Management Area (tertiary catchments T52 and tertiary catchment T40) water resource zone. All the rivers within the study area drain to the south, into Umtamvuna River which forms the southern part of the study area, and ultimately flows into the Indian Ocean (Figure 2-3).

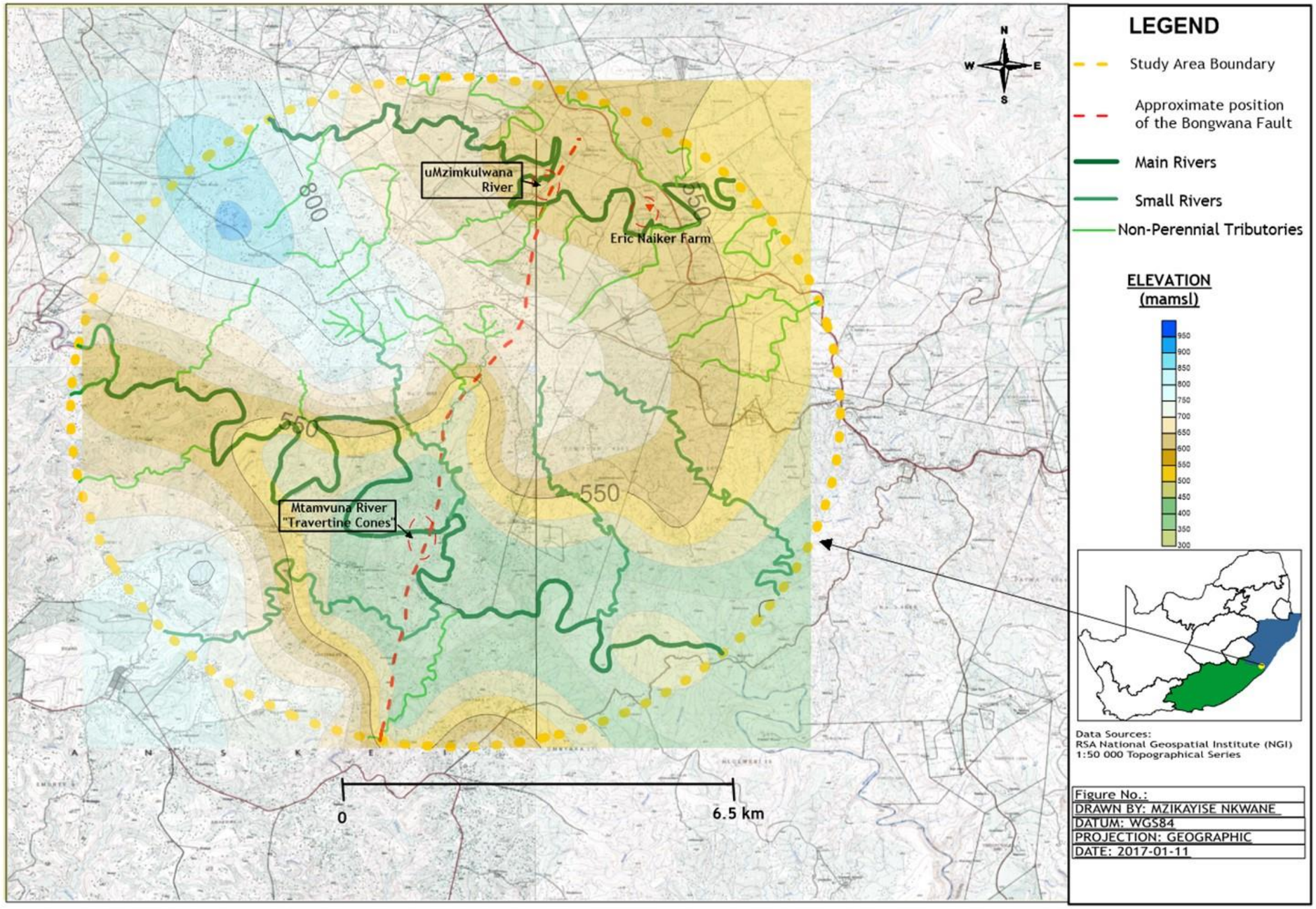

Figure 2-3: Drainage map of the study area

2.3 Geological setting

The regional geology of the Bongwana region is represented by lower Karoo Dwyka Group rocks made up of diamictites, tillites and minor shales, sandstones and conglomerates, which are typical fluvio-glacial environments belonging to the late Carboniferous to early Permian Dwyka Group. Figure 2-4 is a generalized geological map of the study area. The Dwyka Group in the south of the study area rest unconformably or paraconformably on the Cape Supergroup while on the east it unconformably overlies the Msikaba Formation and Natal Group (Johnson et al., 1997).

The deposition of these Dwyka sediments took place when Gondwana migrated over the South Pole during the Carboniferous age (Botha, 1998). The diamictites of the Dwyka Group are highly compacted and generally consists of angular to rounded clasts of the basement rocks embedded in a clay and silt matrix.The sandstones are generally very fine to medium-grain, massive to ripple-laminated, or medium to coarse grain, trough cross-bedded and immature (Von Brunn, 1994).

The rocks of the Msikaba Formation underlying the Dwyka Group are mainly quartz-rich sandstones with intercalated “grit” and conglomerate layers and lenses (Marshal, 1999). The Msikaba Formation was deposited in high-energy shallow-marine environment on a stable platform (Kingsley, 1975). The Msikaba Formation is mainly present in the Kwazulu-Natal province section of the study area. On the Eastern Cape Province side, the Dwyka Group overlies the Table Mountain sandstones (TMS).

The rocks of the Msikaba Formation and the TMS are underlain by basement rocks belonging to the Natal sub-province of the Namaqua-Natal Belt. The Natal Sub-province is divided into three Terranes, namely: Tugela, Mzumbe and Margate Terranes. The Tugela and Mzumbe Terranes are situated to the north of the study area, while the Margate Terrane occurs in the study area. The oldest rocks of the Margate Terrane comprises of the supra-crustal gneisses of the Mzimkulu Group, which the South African Committee on Stratigraphy (SACS, 1980) subdivided it into the Leisure Bay Formation, the Marble Delta Formation and the Mucklebraes Formation.

The Leisure Bay Formation is dominated by meta-pelitic rocks with subordinate calc-silicate gneisses and is described in detail by Grantham (1984). The meta-pelitic gneisses comprise equigranular, finely banded, biotite–orthopyroxene–garnet gneiss and medium-grained melanocratic, biotite – orthopyroxene – garnet – cordierite gneiss (Mendonidis and Grantham, 2003). The cordierite-bearing gneiss occurs as 50 cm bands within the more common biotite – orthopyroxene – garnet gneiss. The calc-silicate rocks occur as thin, homogeneous layers of diopside, sphene and plagioclase intercalated with the meta-pelites (MacCourt et al., 2006).

The Marble Delta Formation is dominated by carbonate rocks and is described in detail by Otto (1977), who recognises an upper, calcitic ‘‘Oribi’’ member and a lower, dolomitic ‘‘Le Jonquet’’ member. The upper member consists mainly high grade calcite that is exploited for commercial purposes (MacCourt et al., 2006). Common accessory minerals include forsterite, graphite, phlogopite, scapolite and serpentine. Subordinate amphibolite forms a relatively thin zone structurally overlying the calcite-rich upper member (MacCourt et al., 2006). Veins of porphyritic charnockite thought to be part of the Oribi Gorge Suite intrude the upper unit, and wollastonite is locally developed along the intrusion contacts. The lower unit is made of dolomite that is currently being commercially exploited for cement production. It contains diopside, altered to tremolite, and forsterite, altered to serpentine, as common accessory minerals (MacCourt et al., 2006).

The Mucklebraes Formation comprises mafic granulite and calc-silicate rocks (Thomas, 1988). The mafic gneisses are two-pyroxene granulites with calcic plagioclase, biotite and hornblende whereas the calc-silicate rocks carry diopside, garnet and idocrase (McCourt et al., 2006).

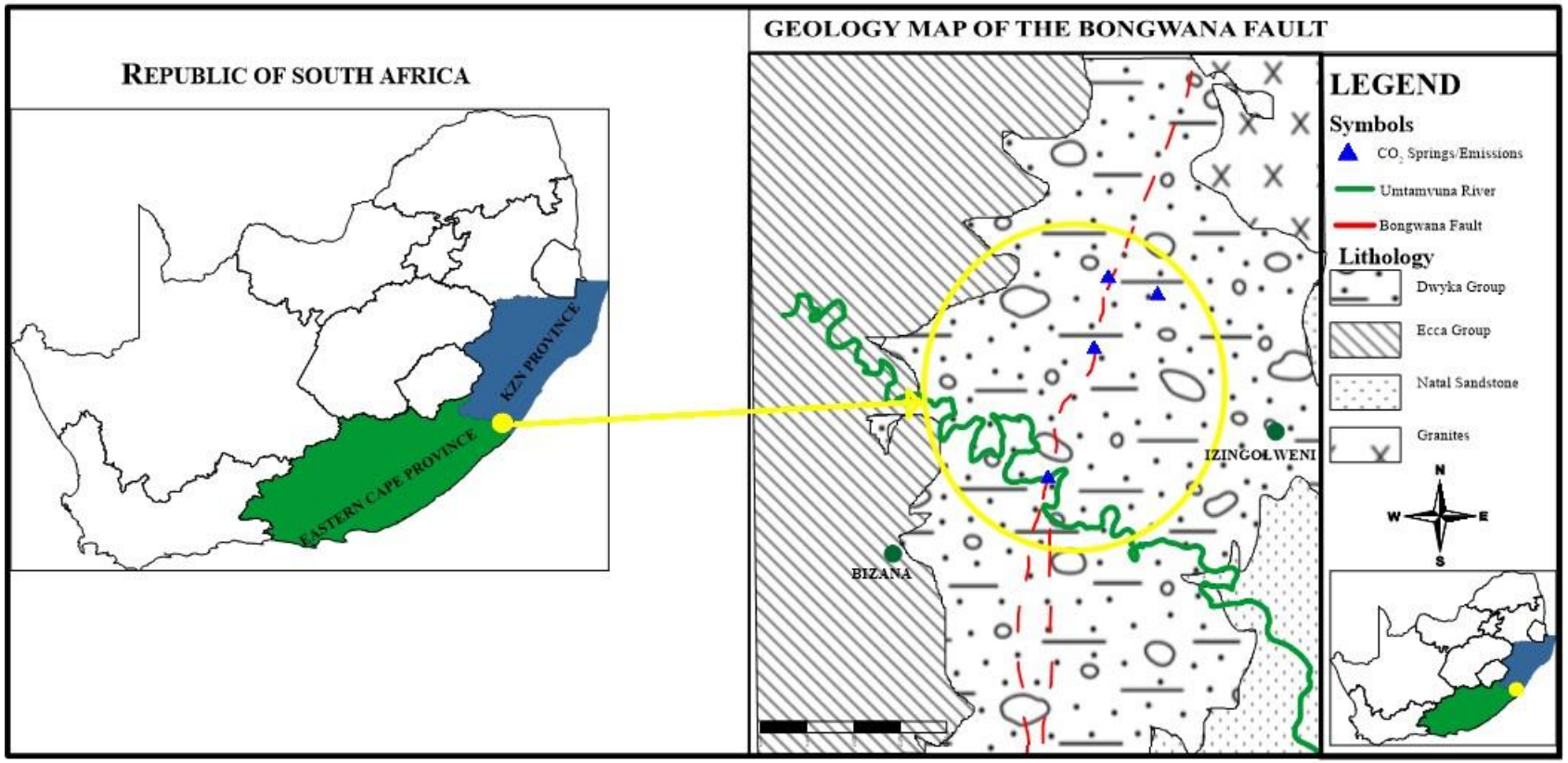

Figure 2-4: Simplified Geology map showing the prevailing geological conditions within the study area (Council for Geosciences, 1988)

2.4 Hydrogeological conditions

The hydrogeological conditions within the study area are controlled by the geology, structure and climate. The surface geology within the study area is dominated by rocks of the Dwyka Group, which is composed of mainly massive tillites, diamictites and minor sandstones and shales. The Dwyka Group rocks exhibit no primary porosity and generally display a very low hydraulic conductivity (WRC, 2002). However, these rocks may exhibit secondary porosity in areas where they have been intruded by Karoo dolerites or when affected by tectonic activity such as faulting.

Underlying the Dwyka Group rocks within the study area are the rocks of the Msikaba Formation. Msikaba Formation comprise the light coloured quartz arenite rocks at its upper part and pale-brownish conglomerate and sandstone at its lower part. Cementation and compaction have decreased the primary porosity in the rocks. Groundwater in the Msikaba Formation is mainly hosted by the secondary porosity.

2.4.1 Aquifer types

The aquifer within the study area is classified as an intergranular and fractured aquifer system with low primary porosity. Groundwater is hosted by secondary porosity created due to fracturing and faulting. According to the hydrogeological map of Durban (King, 1998), the study area is characterized by borehole yields ranging from 0.1 to 0.5 l/s. Since the sandstones associated with the Dwyka Group were deposited mainly under marine conditions, water from these sandstones tends to be saline with EC values exceeding 1000 mS/m (King, 1998). Exploitable aquifers in the Dwyka Group exist in few places, where sand and gravel are dominant or where the Dwyka Group rocks are extensively intruded by dolerite dykes or fractured. Groundwater recharge in the Dwyka Group is very small ranging from 2 to 3 percent of the mean annual precipitation (MAP). Therefore, based on Parsons' (Parsons, 1995) aquifer classification system, the rocks underlying the study area can be classified as minor aquifers.

2.4.2 Groundwater levels and groundwater flow direction

Groundwater level data for the study area was obtained from the Department of Water and Sanitation (DWS) KZN_GRIP database. Groundwater levels range between 10 and 100 m bgl. Boreholes in the northern part of the study area, near Bongwana Station display shallow groundwater levels (10 to 50 m bgl) and boreholes to the southern part of the study area show deep groundwater levels (50 to 100 m bgl). The groundwater level data indicates a strong correlation between groundwater elevation and topographic elevation (Figure 2-5). It is therefore assumed that groundwater flow within the study area mimics the topography. Groundwater level data used to construct the groundwater level elevation is in Appendix A.

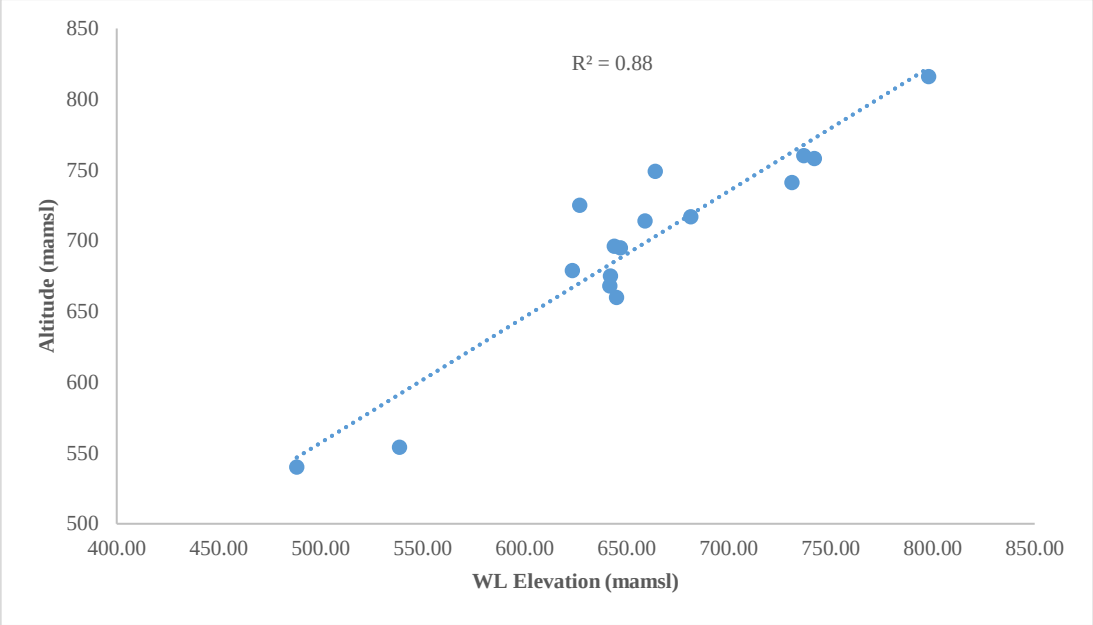

Figure 2-5: Groundwater level elevation vs altitude

2.4.3 General groundwater quality

The available groundwater quality data from the GRIP boreholes suggest that the highest EC and TDS values are 100 mS/cm and 700 mg/l, respectively. The pH values vary between 7 and 8, with most boreholes displaying neutral pH conditions. Trace element concentrations appear to be low throughout the study area. Sodium and calcium appear to be the dominant cations.

3. CHAPTER 3: LITERATURE REVIEW

3.1 Carbon dioxide emissions and climate change

Carbon dioxide is one of the main Greenhouse gases and is the primary contributor in the recent global climate change (IPCC, US EPA). CO_2 is absorbed and emitted naturally as part of the carbon cycle, through plant and animal respiration, volcanic eruptions, and ocean-atmosphere exchange. As part of the natural carbon cycle, people and animals breathe in oxygen from the air and breathe out CO_2. On the other hand, green plants absorb CO_2 for photosynthesis and emit oxygen back into the atmosphere. As a greenhouse gas, its presence in the atmosphere traps heat from the sun. Normally, this keeps the climate warm enough for life to continue. Human activities, such as the burning of fossil fuels and changes in land use, release large amounts of CO_2, which result in the increase in the levels of CO_2 in the atmosphere. The increase in the CO_2 levels in the atmosphere contributes to global climate change (IEA, 2008).

There are numerous techniques that are currently explored to determine ways of curbing the CO_2 emissions into the atmosphere. One of the techniques that are currently perceived as feasible in curbing the CO_2 emissions is the Carbon Capture and Storage (CCS) in deep geologic formation. This technique is widely studied throughout the world. South Africa is looking at employing this technique as an effort to curb the CO_2 impacts in the atmosphere. Two sites in South Africa have been identified with the potential of storing CO_2.

The primary site is the Zululand Group, in the northern KwaZulu Natal areas known as Kwamhlabuyalingana area. The second site is the Algoa Bay in Eastern Cape. The primary concern with the CCS technique in South Africa is lack of monitoring experience since the project is still in a testing phase, hence the Bongwana monitoring project was initiated to counteract this challenge. The following sections elaborate more on the sources of CO_2, its impact on groundwater and CCS technique.

3.1.1 Source of CO_2

Carbon dioxide gas can be derived from both anthropogenic and natural processes by the burning or chemical treatment of organic matter, materials of organic derivation such as coal, oil and the hydrocarbon gases and rocks composed of carbonate minerals.

Anthropogenic sources

According to the Environmental Protection Agency (EPA) in the United States, The main anthropogenic sources of CO_2 is the combustion of fossil fuels (coal, natural gas, and oil) for energy and transportation, although certain industrial processes and land-use changes also emit CO_2. The combustion of fossil fuels to generate electricity is the largest single source of CO_2 emission in the nation. The type of fossil fuel utilized to produce electricity will release different amounts of CO_2. The burning of coal to generate electricity will produce more CO_2 than oil and gas. The combustion of fossil fuels such as gasoline and diesel to transport people and goods also emit significant amounts of CO_2 into the atmosphere. In addition to the energy and transportation sectors as sources of CO_2, many industrial processes emit CO_2 through fuel combustion, however, there are also other processes, apart from combustion, that produces CO_2. These processes emit CO_2 through chemical reactions that do not involve combustion, for example the production and consumption of mineral products such as cement, the production of metals such as iron and steel and production of chemicals (EPA, 2016).

Natural sources

The generation of CO_2 by natural processes occur in a similar manner in which the generation of CO_2 by anthropogenic sources occurs. The generation of CO_2 by natural processes takes place when natural materials containing carbon are subjected to magmatic assimilation, heat generated by faulting, igneous intrusion and metamorphism, the action of acid groundwater on carbonate rocks and the kinds of decay and fermentation that occur during the transformation of buried organic matter into coal and hydrocarbons. Some of the most important natural processes responsible for the generation of CO_2 in the earth's crust are summarised below:

Degassing of magma: most of the naturally occurring CO_2 emitted from the earth crust originates from the degassing of magma. Magma degasses due to the pressure reduction that occurs when magma rises to the earth's surface. This enables the dissolved CO_2 and other gases such as water vapour to be released from the solution in the magma and accumulate as free gas. Most of the CO_2 originating from the degassing of magma is released through volacanoes and associated fissures or hydrothermal sites such as one Yellowstone National Park in the USA (BGS, 2005).

Contact metamorphism of carbonate rocks: magma does not always daylight onto the earth surface. Sometimes it intrudes into the sedimentary rocks and crystallises at depth as plutons or dykes and sills. The heating and metamorphism of carbonate rocks by magmatic intrusions may result in carbonate rocks being metamorphosed into oxides and hydroxides and will give off CO_2, this process is similar to the calcination of limestone in cement manufacture. The process of heating and metamorphism of the host rock by intrusions is known as contact metamorphism.

Thermal maturation of type III (coaly) kerogen and coals: Kerogens are organic chemical compounds generated from the plant and animal organic matter that becomes incorporated in sediments. Rocks with elevated quantities of kerogen are known as petroleum source rocks. Most source rocks are mudstones and shales that contain a few amounts of finely dispersed kerogen while some source rocks, known as oil shales may contain large amounts of kerogen. As kerogen rich rocks become buried deep in the earth crust in actively subsiding sedimentary basins, they are converted into other compounds by increasing heat and pressure during a process called maturation. During maturation process, kerogen-rich rocks give off volatiles such as water, methane, CO_2 and the compounds that make up crude oil.

Biogenic Breakdown of oil and gas: Carbon dioxide may also be formed by the breaking down of oil and gas. The good example of this is the oil that is leaking from a salt diaper in the Central North Sea is biodegrading as it moves upwards and converted to carbon dioxide (Cody et al., 1999; Clayton et al., 1997). $\delta^{13}C_{CO_2}$ values vary between -43.9 to -34‰ which is indicative of biodegradation process (BGS, 2005).

Regional metamorphism of carbonate rocks: Regional metamorphism affects broad areas of the crust, such as places where plates once collided and mountain belts formed. It results from the burial of rocks to sufficient depths within the earth for the temperature and pressure to change their mineral composition. It has been proposed that regional metamorphism of limestone could result in the generation of CO_2 in a similar manner to contact metamorphism.

3.1.2 Migration of CO_2 in the earth's crust

Carbon dioxide formed at depth beneath the earth's crust tend to migrate upwards towards the earth's surface because it is lighter (BGS, 2005). Most of the CO_2 generated in natural systems does not encounter suitable subsurface structures that could trap it and so it is able to migrate both laterally and vertically along permeable pathways. These pathways could be layers of porous and permeable sedimentary rocks, such as sandstones, and/or fractures and fissures that cut through both permeable and otherwise less permeable rocks. The migration of CO_2 in the rocks is in many ways similar to that of natural gas such as methane. When CO_2 gas permeates through the rocks gas flow tend to be concentrated along any fault or fissures that may be present, or along the outcrop of porous and permeable sedimentary rocks. (BGS, 2005). Most rocks at shallow depths of a few tens of meters or less contain fractures such as joints and faults that are open and highly permeable.as a result, in many natural CO_2 emission sites the CO_2 tends to flow along these fractures. Although CO_2 does not necessarily escape along the entire length of a fracture or fault, it will tend to emerge at one or more discrete points along the fault or fracture. The reason for this is that the permeability along the fault length varies and once the breakthrough occurs at one point, a channeling effect will occur.

In an offshore environment, the movement of gases through the sea bed commonly produces pits called “pockmarks. In some instances, CO_2 emerges at the sea bed dissolved in water or as a free gas. If in a free gas phase it may form a train of bubbles that will rise through the water column. In onshore sedimentary basins, migrating CO_2 will pass through two hydrogeological zones on its way to the surface. Most of it passage will be through the lower saturated zone, below the water table, where pore spaces, and any fractures found within the rocks are fully saturated with water. The unsaturated zone above the water table is largely filled with soil gas. Once CO_2 emerges through the saturated zone it will tend to disperse within the unsaturated zone. It may pool on top of the water table and disperse laterally before emerging at the ground surface.

The other way in which naturally occurring CO_2 typically appears from the ground in onshore sedimentary basins is in carbonated springs. These occur when CO_2 has dissolved in groundwater in the saturated zone. The example of such springs are found in France. In some countries, these have been used as sources of drinking water.

3.1.3 Impacts of dissolved CO_2 on water chemistry

Studies of the impacts of CO_2 from the CO_2 sequestration sites reveals that the dissolution of CO_2 in groundwater to form carbonic acid and its subsequent dissociation causes a decrease in pH. Acidic pH conditions in groundwater promotes the dissolution of carbonate rocks such as calcite according to the following mass balance reactions:

$$CO_{2\,(g)} = CO_{2\,(aq)} \quad (1)$$

$$CO_{2\,(aq)} + H_2O = HCO_3^- + H^+ \quad (2)$$

$$CaCO_3\ (\text{calcite}) + H^+ = Ca_2^+ + HCO_3^- \quad (3)$$

Changes in pH and the production of HCO_3^- will influence or control the dissolution of minerals and the subsequent release of chemical elements and contaminants into the aqueous phase, as well as precipitation reactions and formation of neophases. In addition, these changes may significantly affect the extent and rate of chemical, biological, and hydrological processes and reactions, which may control contaminant mobility in the subsurface.

Experimental and modeling studies indicate that CO_2 intrusion into the vadose zone or potable aquifers could induce a decrease in aqueous pH of 1 to 3 units (Little and Jackson, 2010; Lu et al., 2010; Wang and Jaffe, 2004; Wilkin and DiGiulio, 2010; Zheng et al., 2009; Kharaka et al., 2010). Decreases in pH well-buffered systems where CO_2-induced dissolution of reactive carbonates (Equation 4), feldspars (Equation 5), and/or the dissolution/precipitation of clays (Equation 3 and 4) provide enough buffering capacity (via $HCO3^-$ alkalinity) to resist drastic changes in pH.

$$CaCO_3 + CO_2\,(g) + H_2O \rightarrow Ca_2^+ + 2HCO_3^- \quad (4)$$

$$2NaAlSi3O_8 + 11H_2O + 2CO_2\,(g) \rightarrow Al_2Si2O_5\,(OH)_4 + 2Na+ + 2HCO3^- + 4H_4SiO_4 \quad (5)$$

$$Al_2Si_2O5\,(OH)_4 + 5H_2O + 6CO_2(g) \rightarrow 2Al_3^+ + 6HCO_3^- + 2H_4SiO_4 \quad (6)$$

This suggest that rocks containing carbonate minerals can effectively buffer the acidity associated with the dissolution of CO_2 in groundwater. The dissolution of calcite takes place as long as there is enough CO_2 dissolving in groundwater. When there is no more dissolving CO_2 in groundwater, groundwater eventually becomes saturated with respect to calcite and will no longer be able to dissolve the rock. Furthermore, when the CO_2-rich groundwater gets into the surface, CO_2 is released into the atmosphere and the dissolution of calcite drops. When the CO_2 is lost, the solubility of calcite drops and calcite crystallizes from water. This is the mechanism by which specleothems (Stalactites etc) grow within caves, or travertine (calcite crusts) are formed at surface.

Poorly buffered systems (e.g., sandy soils in aquifers) are devoid of sufficient quantities of alkalinity producing minerals and therefore lack the ability to resist changes in pH. In such systems, the decrease in pH due to the dissolution of CO_2 into solution is generally more apparent and the risk for pH-induced perturbation to environmental quality is more significant and prolonged compared to well-buffered systems (McGrail et al., 2006; Wang and Jaffe, 2004; Wilkin and DiGiulio, 2010).

3.1.4 Technique to curb CO_2 release: Carbon Capture and Storage (CCS)

CCS is defined as the process of capturing CO_2 from large emission sources and injected, in a supercritical state, normally into deep geological formations that are capable of storing the CO_2 almost permanently without release from the storage formation (Lemieux,2011) and has been deemed as a promising alternative for reduction of greenhouse gas emission. Successful geologic storage of CO_2 requires storage capacity with high effective porosity in the geological formation and should be feasible of high injection rate of CO_2. Concurrently, there should be a confining layer on top of the permeable geological formation to prevent CO_2 from migrating outside of the rock formation. The existence of this confining layer on top of the permeable saline aquifer is primary requirement for the CO_2 storage facility in deep geological formations. For successful confinement, the injected CO_2 should be trapped physically, chemically, or mineralogically.

The fate of the injected CO_2 and its effects on the chemical changes of groundwater quality have been extensively proposed and discussed through laboratory (Little and Jackson, 2010; Lu et al., 2010; Frye et al., 2012; Terzi et al., 2014) and field tests (Kharaka et al., 2010; Cahill et al., 2014). It has been understood that dissolved CO_2 in groundwater has potential to degrade the shallow depth groundwater quality (Bachu, 2008; Newmark et al., 2010; Harvey et al., 2012; Siirila et al., 2012). Thus, although it is challenging, development of detection system in a shallow aquifer region is crucial to assure the long term safety of the injected CO_2 in deep saline aquifers. The previous CCS cases show that continuous monitoring of pH, EC, TDS and major cations and anions concentration is the most basic and important factor for leakage detection. Trace elements and isotopes are also widely used to determine the CO_2 leakage.

The integrated technological CCS process consists of the separation of CO_2 from industrial and energy-related sources, transport to a storage location and long-term isolation from the atmosphere. There are three main approaches that are employed in CCS, namely: Pre-combustion, Post-combustion and Oxyfuel combustion (IPCC, 2005). Figure 3-1 below shows schematic representation of the processes involved in the CCS.

1) Pre-combustion

Pre-combustion CCS takes place before the fuel (normally coal or natural gas) is placed in the furnace by first converting coal into a clean-burning gas and separating the CO_2 released by the process. For coal, the pre-treatment involves a gasification process conducted in a gasifier under low oxygen level forming a syngas which consists mainly of CO and H_2, and is mainly free from other pollutant gases.

The syngas will then undergo water gas shift reaction with steam forming more H_2 while the CO gas will be converted to CO_2. The following reaction equations illustrate the process of CO_2 separation by pre-combustion method.

$$Coal \xrightarrow{Gasification} CO + H_2 \quad (7)$$

$$CO + H_2O \xrightarrow{Water-Gas\ Shift} H_2 + CO_2 \quad (8)$$

Natural gas, as it mainly contains CH4, can be reformed to syngas containing H_2 and CO.

$$CH_4 + H_2O \xrightarrow{Reform} CO + H_2 \quad (9)$$

The content of H_2 can be increased by the water gas shift reaction (Eq. (8)) and the rest of the process is similar to that described above for coal.

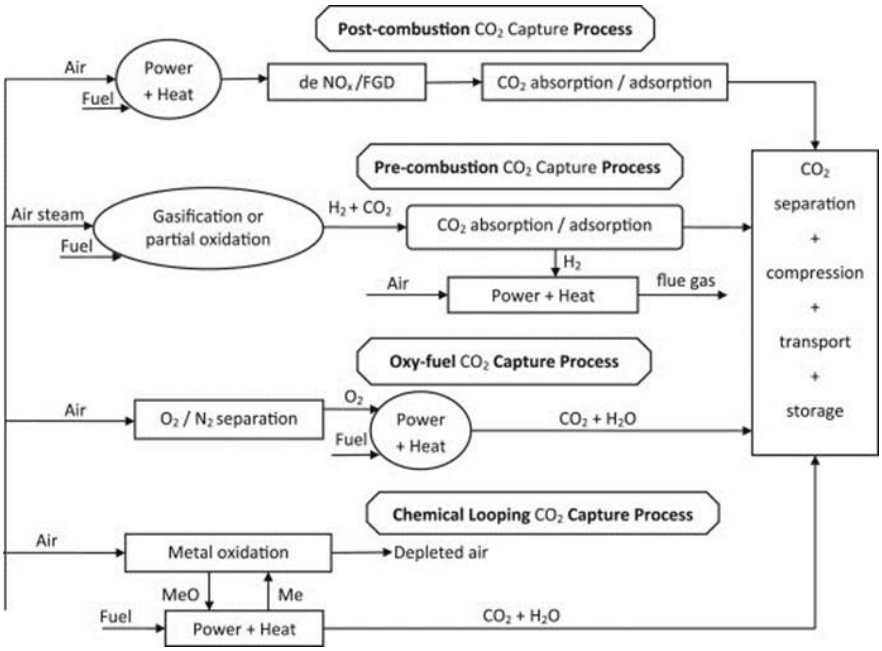

Figure 3-1: Schematic representation of the processes involved in CCS.

2) Post-combustion

In the post-combustion method, CO_2 is separated from the flue gas of the power station by bubbling the gas through an absorber column packed with liquid solvents (such as ammonia) that preferentially take out the CO_2. In the most commonly-used techniques, once the chemicals in the absorber column become saturated, a stream of superheated steam at around 120°C is passed through it. This releases the trapped CO_2, which can then be transported for storage elsewhere.

3) Oxyfuel combustion

Oxyfuel combustion systems use oxygen instead of air for combustion of the primary fuel to produce a flue gas that is mainly water vapour and CO_2. This results in a flue gas with high CO_2 concentrations (greater than 80% by volume). The water vapour is then removed by cooling and compressing the gas stream. Oxyfuel combustion requires the upstream separation of oxygen from air, with a purity of 95–99% oxygen assumed in most current designs. Further treatment of the flue gas may be needed to remove air pollutants and non-condensed gases (such as nitrogen) from the flue gas before the CO_2 is sent to storage. As a method of CO_2 capture in boilers, oxyfuel combustion systems are in the demonstration phase (see Table TS.1). Oxyfuel systems are also being studied in gas turbine systems, but conceptual designs for such applications are still in the research phase (IPCC, 2005).

4) Transportation

When the storage site is not located directly next the emission sources, as in the case of South Africa, the captured CO_2 needs to be transported. Pipelines have been used for this purpose in the USA since the 1970s. CO_2 could also be transported in liquid form in ships similar to those transporting liquefied petroleum gas (LPG). For both pipeline and marine transportation of CO_2, costs depend on the distance and the quantity transported. For pipelines, costs are higher when crossing water bodies, heavily congested areas, or mountains.

5) Storage

CO_2 can be stored into geological formations such as deep saline aquifers which have no practical use, and or gas reservoirs. Geological storage is at present considered to be the most viable option for the large CO_2 quantities needed to effectively reduce global warming and related climate change (Leung, 2014). Deep ocean storage is also a feasible option for CO_2 storage although there are environmental concerns such as ocean acidification and eutrophication that are most likely to limit its application. The research shows that deep saline aquifers can stored large amounts of CO_2 gas than depleted oil and gas fields.

Studies in the Zululand basin are currently underway to assess the feasibility of storing CO_2 in deep saline aquifers of the Zululand Group. The Zululand basin forms a potential onshore target for CCS in South Africa, located on the east coast of South Africa in the northern KwaZulu-Natal Province.

The basin represents an onshore extension of the southern Mozambique Basin, with basin-fill sediments of late Barremian to late Maastrichtian age (Chabangu et al., 2014). The Zululand Basin comprises the rocks belonging to the Zululand Group. Six sandstone packages with varying reservoir properties were identified in the Zululand Basin (Chabangu et al., 2014), however due to depth restrictions for CCS only two were investigated. The basal, Aptian-aged sandstone identified in the Makatini Formation represents the lower potential reservoir whilst a sandstone succession of upper Cenomanian- to Turonian-age represents the uppermost sandstone unit of the Makatini Formation and the lowermost sandstone unit of the St Lucia Formation. Both reservoir packages are well developed at the Kosi Trough.

3.2 Previous studies on the Bongwana fault

Natural CO_2 springs at the Bongwana area were first studied in the early 20th century by Young (1923) and Gevers (1941). Further work conducted by Gevers (1941) and Du Toit (1946) led to the identification and characterisation of the other CO_2 springs associated with the deposition of the travertine cones near Umtamvuna River, south of the Bongwana area. These CO_2 springs were believed to be associated with an 80km long N-S trending fault known as Bongwana fault (Harris, et al., 1997). Young (1923) stated that CO_2 gas emanates from fault fissures in the Dwyka tillites, indicated in the surface by silicified wall rock. Analysis of the fresh and kaolinised Dwyka tillites showed 65.49 % and 75.21% silica, 14.82% and 16.63% Al_2O_3 respectively. Appreciable amounts of calcite and magnesium were also observed as CaO (2.99%) and MgO (2.79%). CO_2 samples obtained by Young (1923) (published in Gevers 1941) returned CO_2 percentages of 98.3% and 97.6% for 2 samples, each with O_2 content of 0.2%, and N_2 (by difference) of 1.5% and 2.2% respectively. The analysis of the carbon and oxygen isotopes for Bongwana CO_2 gas exhalations done by Harris et al., (1997) from seven locations in the Bongwana area ranged from -0.98 to 0.85‰ for $\delta^{13}C$ and from 35.31 to 45.06‰ for $\delta^{18}O$. The analysis of the travertine rocks samples near Umtamvuna River published by Gevers (1941) indicated high calcite (41.85%) as CaO and iron (14.64%) as Fe_2O_3. Appreciable amounts of silica (1.43%) and magnesium (1.73%) as MgO were also reported. Two models were proposed for the CO_2 generation along the Bongwana fault. The model proposed by Gevers (1941) suggested that CO_2 is generated at depth by the reaction of groundwater and carbonate rocks. The second model proposed by Hartnady (1985) suggest a magmatic source of the CO_2. The carbon and isotope data published by Harris et al., (1997) for CO_2 gas from the Bongwana fault indicated carbonate source for CO_2 generation in favour of the Gevers model. According to Gevers (1941) groundwater from the travertine cone springs originate from the Dwyka Group (local recharge) and percolate to greater depth. However, no isotope data to support this, the assumption was based on the fact that the two groundwater sources exhibit the same temperatures.

4. CHAPTER 4: RESEARCH METHODOLOGY

The information presented in this research was generated during the course of the research field observations and testing, and also collected from various sources on a desktop level study. The information gathered was then analysed using dedicated hydrogeological software packages and presented in the form of tables, graphs and diagrams. A hydrogeological conceptual model was then proposed based on the results of the analyses of all information.

4.1 Data collection

The data in this study was collected by undertaking a desktop survey as well as a literature review of all available information regarding the research topic. The field assessment was undertaken to map the study area, conduct a hydrocensus and collect water samples for hydrochemical and isotope analysis. The field water quality parameters were measured during the field assessment.

4.1.1 Desktop study

The desktop study was undertaken by assessing all the available information on the topography, rainfall, drainage, geology and hydrogeology of the study area. The following data sources were used:

- 1:250 000 Geological Map Series: 3030 Port Shepstone, prepared by Council for Geosciences;
- 1:250 000 Geological Map Series: 3028 Kokstad, prepared by Council for Geosciences;
- 1:250 000 Geological Map Series: 3128 Umtata, prepared by Council for Geosciences;
- 1:500 000 Hydrogeological Map Series of the Republic of South Africa, Durban area, prepared by King (1998);
- Google Earth images;
- Department of Water and Sanitation (DW&S) 2016 KZN GRIP data;
- CHART database compiled by the Department of Water and Sanitation.

4.1.2 Literature review

The literature review was done on all available information from previous studies conducted on the impacts of CO_2 on groundwater and surface water resources. The literature review included, but was not limited to, studying of papers, articles and books on the origin of CO_2 from natural and anthropogenic processes, sequestration of carbon dioxide in deep geological formations and related water quality issues associated with CO_2 leakage from the storage site. The papers from the previous studies conducted by Gevers (1941), Du Toit (1946), De Decker (1981) and C. Harries (1997) on the Bongwana fault and associated CO_2 emissions were obtained and used to inform the desktop assessment. In addition to the above, available methods of capturing and transporting CO_2 from the source area to a storage facility and the suitability of the geological formation for storing CO_2 were studied as well.

4.1.3 Data consolidation

All the data collected from the desktop study and literature review was merged together and the site maps were constructed for the field assessment phase. Target areas for hydrocensus and sampling were delineated based on the desktop assessment results. The literature review results were used to decide the hydrochemical determinants to be analyzed from the samples collected in the field which will indicate the impacts of CO_2 on groundwater and surface water quality.

4.2 Field assessment

The field work was undertaken in stages as described below. The preliminary field assessment was done in collaboration with the South African Centre for Carbon Capture and Storage (SACCCS), Council for Geosciences (CGS), Council for Scientific Industrial Research (CSIR), British Geological Survey (BGS) and the University of Edinburgh (*School of Geosciences)* in the UK. The objective of the site visit was mainly to locate the CO_2 sites and measure CO_2 emissions (CSIR), undertake soil gas measurements (British geological Society), fault mapping (University of Edinburgh) and obtain preliminary water quality field parameters (Council for Geoscience).

4.2.1 Preliminary field assessment

A preliminary visit to the study area, organized by the South African Center for Carbon Capture and Storage, was conducted from the 19th of September 2015 for a week and

during the duration of the excursion areas along the Bongwana Fault, where CO_2 release have been identified, were visited (refer to photos below from Photo No: 1 to Photo No: 8). The areas visited include Umzimkulwana River, a borehole with CO_2 emission in a farm about 4km from Umzimkulwana River, Umtamvuna River and Mbangweni River. Preliminary water quality field parameters were measured from the CO_2 sites and used to plan a detailed hydrocensus and field sampling protocol for further hydrochemical analysis.

4.2.2 Hydro-census and sample collection

Following the results of the preliminary site assessment, a detailed hydrocensus was conducted approximately 10km on either sides of the Bongwana fault. GRIP boreholes located within this range were visited, sampled and GPS co-ordinates were obtained for the construction of sampling maps. Sample collection was done according to the methodology outlined by the Water Research Commission (WRC) for major cations and anions, trace metals and isotopes. Samples were filtered on site and kept in cooler boxes before transported to the laboratory for hydrochemical analysis. Prior to any groundwater sampling in boreholes the static water rest levels, in meters below ground level (m bgl), were measured, where possible, and recoded.

4.2.3 Field measurements

Water quality field parameters were measured using a HI9829 waterproof portable logging multiparameter meter that monitors several in situ water quality parameters. The microprocessor based multi-sensor probe allows for the measurement of key parameters including electrical conductivity (EC), total dissolved solids (TDS), pH, temperature, dissolved oxygen (DO), Eh and ORP.

An in situ titration was performed in the samples in accordance with the methodology suggested by Snoeyink and Jenkins (1980). A volume of 100ml of the sample collected was used to titrate the sample using hydrochloric acid and Phenolphthalein indicator to a pH of 4.5 to determine the total alkalinity of the sample. The total volume of hydrochloric acid used to reach the pH end point was recorded and used to calculate the total alkalinity and bicarbonate concentration using the following formula suggested by Snoeyink and Jenkins (1980).

Photo No: 1
Sample No: BGN-15

Photo No: 2
Sample No: BGN-16

Photo No: 3
Sample No: BGN-12

Photo No: 4
Sample No: BGN-11

Photo No: 5
Sample No: BH1

Photo No: 6
Sample No: BGN-20

4.3 Laboratory analysis

The laboratory hydrochemical analysis was carried out in the Council for Scientific and Industrial Research (CSIR) inorganic laboratory in Pretoria. Samples were analyzed using ELAN 6100 Inductively Coupled Plasma Mass Spectrometer (ICP-MS) for trace element analysis and an ion chromatograph (IC) for major ion analysis. Environmental isotope samples were analyzed at the iThemba Environmental Isotopes Laboratory following standard procedures. Travertine rock samples were collected from either side of Umtamvuna River. Thin sections were prepared from travertine rock samples collected from Umtamvuna River and analyzed under a polarized microscope. The two travertine rock samples were crushed into a fine powder at the UKZN Geological Sciences laboratory and analyzed using XRD and XRF.

4.4 Data analysis, interpretation and conceptualization

The data obtained from the desktop, field assessment and laboratory analyses are presented in the results section in the form of tables, graphs, piper plot and maps. Aquachem software was used to plot the hydrochemical data on a piper plot diagram to determine the water types and the geochemical software, PhreeqC, was used to determine saturation indices of various mineral phases.

Figure 4-1 shows the flow chart of the methodology used. The flow chart shows the steps that were followed from the data collection phase up to the final stage of the research.

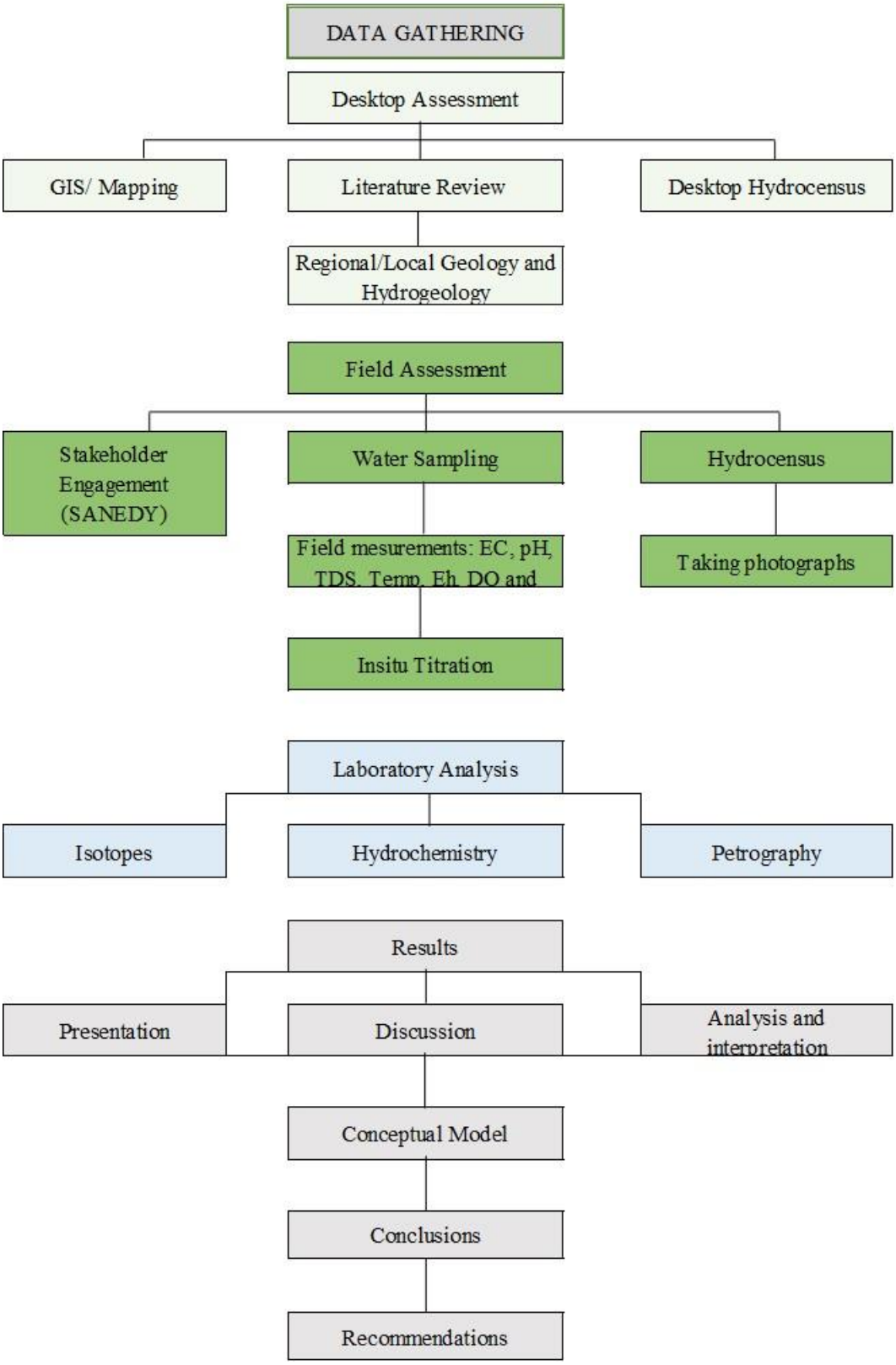

Figure 4-1: A flow chart showing the processes followed during the course of this research

5. CHAPTER 5: RESULTS

The main results of the hydrogeological study along the Bongwana Fault are presented in the following sections.

5.1 Field measurements

In situ water quality parameters such as pH, electrical conductivity (EC), temperature, dissolved oxygen (DO), oxidation–reduction potential (ORP) and total dissolved solids (TDS) measured are tabulated in Table 5-1. The graphs of the pH and EC for the CO_2-rich and CO_2-poor sites are shown in Figure 5-1 and Figure 5-2 respectively. The figures show that lower pH and elevated conductivity values were measured at CO_2-rich sites compared to CO_2-poor sites. The decrease in pH at CO_2-rich sites is evident from Umzimkulwana River in the Bongwana area and Umtamvuna River in Bizana area. Both rivers display high pH (alkaline) upstream of the CO_2 emission and low pH (acidic) at and downstream of the CO_2 emission indicating that CO_2 is responsible for the decrease in pH conditions. However, further downstream of the CO_2 emission sites, the pH increases again to the background pH level of the river. Elevated conductivity values were noted from the travertine cones near Umtamvuna River and in the CO_2-rich borehole. The concentration of the dissolved oxygen measured varies from site to site, however, CO_2-rich sites typically display lower DO concentrations compared to CO_2-poor sites.

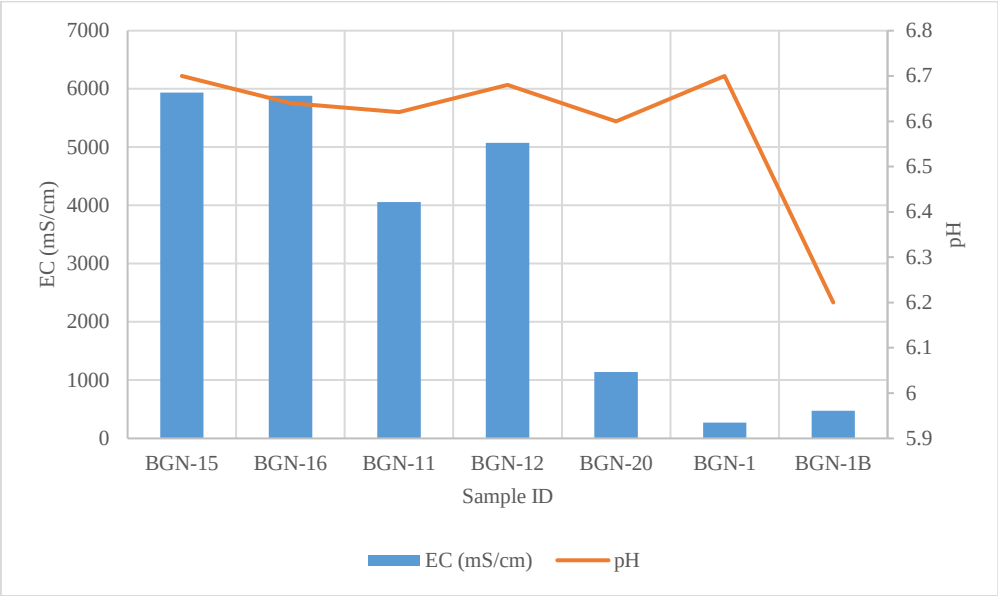

Figure 5-1: Graph of the electrical conductivity versus the pH for CO_2 emission sites

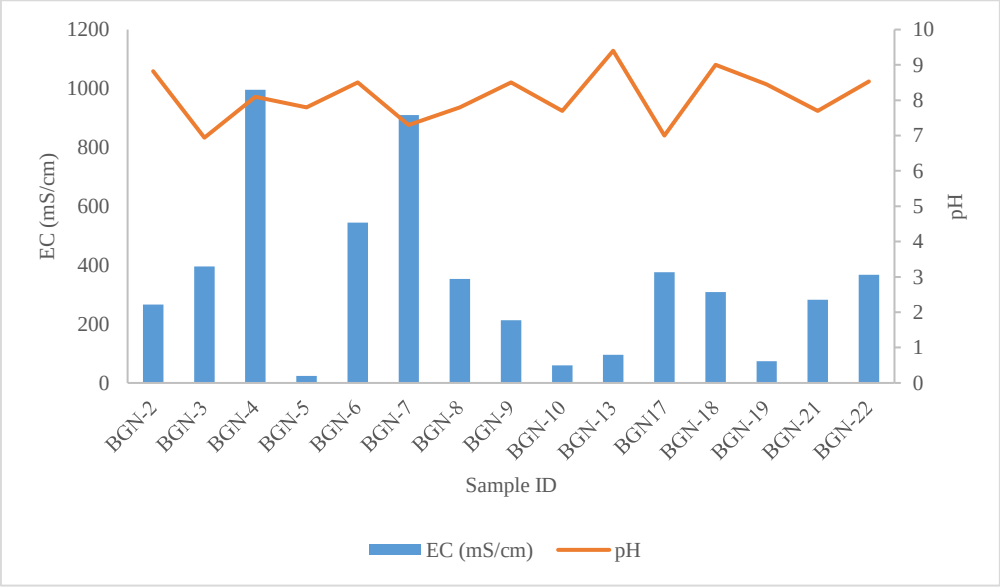

Figure 5-2: Graph of the electrical conductivity versus the pH for sites with no CO_2 emissions.

Table 5-1: I*nsitu* water quality parameters

Sample ID	Site Description	Static Groundwater Level (m bgl)	pH	EC (mS/m)	TDS (ppm)	Temp (°C)	Eh (mV)	ORP	DO (ppm)	TALK (mg/l CaCO3)	Bicarbonate (mg/L HCO_3)	Carbonate-CO_3 (mg/L)
BGN-1	Surface water site at Umzimkulwana River downstream of the small bridge on a dirt road. The site is identified by carbon dioxide gas bubbles from the river bed that issue from an approximately 20m wide fault gouge.	N/A	6.7	269	134	25.18	7.3	24.5	7.7	108	137.7	0
BGN-1B	Small pond near Umzimkulwana river with carbon dioxide gas bubbles. This site is located about 4-5m west of station number 1A.	N/A	6.2	476	352	28.1	40.6	-4.4	5.04	280	341.5	0
BGN-1C	Downstream surface water point at Umzimkulwana river.	N/A	6.72	272	135	25.39	8.5	8.5	7.5	0		
BGN-2	Upstream surface water point at Umzimkulwana river.	N/A	8.82	266	134	24.8	-94	-6.1	7.28	108	124.4	3.8
BGN-3	Borehole located within the Big Bend farm, north of the Bongwana train station, about 300m from the turnoff on the N2 road to Umzimkulwana River through the dirt road.	26.21	6.94	396	206	22.7	-5.5	21.2	3.11	174	212.1	0.1
BGN-4	Borehole fitted with a hand pump next to the N2 road from Izingolweni town to Harding.	N/A	8.1	996	552	19.88	-62	-82.2	2.5	317	382.2	2.2
BGN-5	Oribi Gorge Hotel rain sample	N/A	7.8	24	15	15.2	-54	-11.4	8.76		-	-
BGN-6	Ugu district Municipality borehole fitted with hand pump (UGU EZ1010).	N/A	8.5	544	308	18.88	-160	-116	5	224	265.4	3.9
BGN-7	Borehole equipped with a hand pump used for community water supply.	N/A	7.3	910	504	19.8	-38	-2.6	4.1	279	339.7	0.3
BGN-8	Borehole equipped with a hand pump used for community water supply.	N/A	7.8	353	200	18.8	-69	-24	6	98	118.9	0.3

Sample ID	Site Description	Static Groundwater Level (m bgl)	pH	EC (mS/m)	TDS (ppm)	Temp (°C)	Eh (mV)	ORP	DO (ppm)	TALK (mg/l CaCO3)	Bicarbonate (mg/L HCO_3)	Carbonate-CO_3 (mg/L)
BGN-9	Borehole equipped with a hand pump used for community water supply.	N/A	8.5	213	123	17.98	-86	137	3.85	123	145.7	2.1
BGN-10	Borehole equipped with a hand pump not used.	N/A	7.7	69/60	35	17.73	-83	-195	3.4	0	-	-
BGN-11	Travertine cone north of Umtamvuna River, on the KZN side.	N/A	6.62	4060	2244	19.94	-7.5	-39	1.69	1146	1397.6	0.3
BGN-12	Spring on the banks of Umtamvuna River on the KZN side.	N/A	6.68	5072	2804	19.97	10.5	-49	0.67	1330	1621.9	0.4
BGN-13	Upstream surface water point at Umtamvuna river.	N/A	9.4	96	52	21.34	-146	-45	6.8	0	-	-
BGN-14	Umtamvuna River sample site at the carbon dioxide bubbles.	N/A	7.07	155	83	21.51	-10.1	-9.2	6.49	60	73.1	0
BGN-15	Active travertine cone (T01) south of Umtamvuna River on the eastern cape side.	artesian	6.7	55937	3271	20.14	-12.3	43.5	1.5	1397	1703.5	0.4
BGN-16	Small travertine cone next to the active cone.	artesian	6.64	5884	3233	20.28	7.4	-24.9	2.35	1395	1701.2	0.3
BGN-17	Spring at kwaNdunge community.	N/A	7		214	18.6	-4.5	-27.8	4.73	68	82.9	0
BGN-18	Spring at Dindini community.	N/A	9	309	151	26.2	-130	-18	11.25	0	-	-
BGN-19	Upstream surface water point at Umtamvuna River north of the bridge on the dirt road from Bizana to Harding.	N/A	8.45	74	39	22.1	-95	-24.5	8.9	0	-	-
BGN-20	Borehole within Eric Niaker's farm	15.34	6.6	1137	630	19.88	4	-70	0.64	193	235.4	0
BGN-21	School borehole	35.51	7.7	282	156	19.98	-101	-163	2.9	121	146.9	0.3
BGN-22	Borehole at Mzinhlanga Primary School	N/A	8.53	367	192	22.6	-83	6.7	6.8	167	197.9	2.9

5.2 Water quality and hydrochemistry

Table 5-2 below shows water quality and hydrochemistry results for the samples collected around the study area. The results are compared against the 2015 SANS241-1 South African Drinking Water Standards to determine their suitability for drinking purposes. The values with light red fill exceed SANS241-1 for chronic and acute health and the values with the yellow fill exceed SANS241-1 for aesthetic impact. It can be noted that groundwater in the study area has naturally elevated conductivity, exceeding the aesthetic limits for SANS241-1 Standard, which is typical of the Dwyka Group aquifers. However, groundwater from the travertine cone springs has high TDS and EC values exceeding the normal values measured within the Dwyka Group groundwater. The hydrochemical parameters from the CO_2-rich sites that do not comply with SANS 241-1 limits are iron, manganese and sodium. Although the concentration of the other parameters such as chloride, fluoride and sulphate are within the allowable limits, their concentrations are higher compared to CO_2-free sites. None of the hydrochemical parameters from CO_2-free sites displayed elevated concentrations above the SANS241-1 limits. The concentration of the trace elements from the CO_2-rich travertine cones are higher compared to CO_2-free boreholes, rivers and springs. The results of the trace elements analyzed are shown in appendix B.

The hydrochemical data for groundwater was plotted on a Piper trilinear plot (Piper, 1953), which is the most commonly used method for identifying hydrochemical patterns of major ion composition (Figure 5-3).With respect to cations, most of the samples are scattered in the lower-left triangle, indicating that some are calcium type, some are sodium-type water but most are of a mixed type. Regarding anions, most groundwater samples are plotted in the lower-right zone of the triangle, showing that bicarbonate-type water is predominant. Groundwater from all travertine cone springs are characterized by Na-Ca-Mg-HCO_3 water types, while shallow groundwater from boreholes and river samples show Ca-Na-Mg-HCO_3 types (Table 5-3).

Table 5-2: Major cations and anions

Determinant	Units	SANS241:2015	BGN-1	BGN-2	BGN-3	BGN-4	BGN-6	BGN-7	BGN-8	BGN-9	BGN-11	BGN-12	BGN-14	BGN-15	BGN-16	BGN-17	BGN-20	BGN-21	BGN-22
pH	pH. Units	≥ 5 to ≤9.7	6.7	8.82	6.94	8.1	8.5	7.3	7.8	8.5	6.62	6.68	7.07	6.7	6.64	7	6.6	7.7	8.53
EC	mS/m	≤170	269	266	396	996	544	910	353	213	4060	5072	155	55937	5884	376	1137	282	367
TDS	mg/l	≤1200	134	134	206	552	308	504	200	123	2244	2804	83	3271	3233	214	630	156	192
Barium	mg/L Ba	≤0.7	0.17	0.14	0.30	0.07	0.07	0.07	0.07	0.06	0.05	0.05	0.02	0.08	0.07	0.08	0.17	0.11	0.05
Calcium	mg/l		16	16	33	36	31	40	18	28	269	306	10	336	337	20	30	19	35
Iron (Fe)	mg/L Fe	≤ 2.0	0.15	0.17	0.02	0.34	0.08	0.11	0.02	0.67	0.03	17.54	0.55	15.59	12.71	0.02	4.50	0.03	0.03
Magnesium (Mg)	mg/l Mg		12	12	24	27	35	34	17	9.4	106	120	8.6	133	133	18	46	8.8	12
Manganese (Mn)	mg/L Mn	≤ 0.4	0.039	0.032	0.001	0.124	0.020	0.033	0.002	0.038	0.692	0.707	0.032	0.745	0.744	0.001	0.368	0.073	0.002
Potasium (K)	mg/l K		2	1.9	0.66	1.4	0.58	1.3	0.96	0.26	28	35	1.3	41	41	1.3	3.5	0.77	0.67
Silicon	mg/l Si		7.9	7.9	29	8.6	15	13	17	5.8	6.7	5.9	6.6	5.2	5.2	13	15	18	13
Sodium (Na)	mg/l Na	≤ 200	29	27	28	184	62	114	46	19	697	897	21	1095	1103	14	177	43	43
Brominde	mg/l Br		0	0	0	0.3	0	0.3	0	0	0.2	0.2	-	0.2	0.2	-	0.4	0	0
Chloride	mg/l Cl	≤ 300	31	31	39	91	60	94	61	12	105	111	23	113	114	110	167	40	32
Flouride	mg/l F	≤ 1.5	0.2	0.2	0.47	1.4	0.59	0.53	0.25	0.2	0.35	0.37	0.2	0.29	0.29	0.27	0.49	0.32	0.34
Nitrate Nitrogen	mg/l N	≤ 11	0.2	0.2	2.1	0.45	12	2.1	5.6	0.2	0.2	0.2	0.2	0.2	0.2	0.2	0.2	0.2	0.36
Sulphate	mg/l SO4	≤ 250	5	5	5	10	7.9	5	5	7.6	42	46	7.3	48	50	5	5	5	8.5

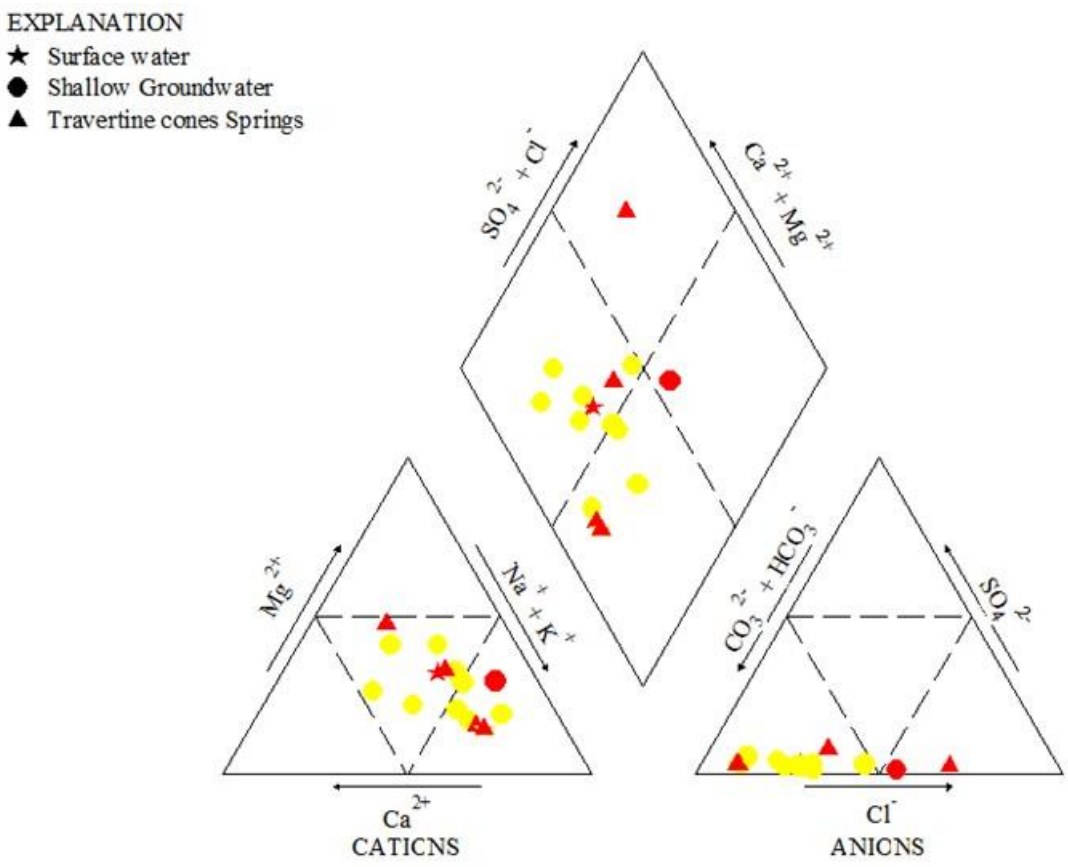

Figure 5-3: Piper plot of the major cations and anions composition for groundwater and surface water samples. The red colour shows CO_2-rich sites and yellow colour shows CO_2-poor sites.

Table 5-3: Hydrochemical facies (water types) for water samples analysed in the study area.

Station ID	Location	Sampling point	Water Type	CO_2-rich
BGN-1	Umzimkulwana River	Surface water	Na-Mg-Ca-HCO3-Cl	Yes
BGN-11	Umtamvuna River	Groundwater	Na-Ca-Mg-HCO3	Yes
BGN-12	Umtamvuna River	Groundwater	Na-Ca-Mg-HCO3	Yes
BGN-14	Umtamvuna River	Surface water	Na-Mg-Ca-HCO3-Cl	No
BGN-15	Umtamvuna River	Groundwater	Na-Ca-Mg-HCO3	Yes
BGN-16	Umtamvuna River	Groundwater	Na-Ca-Mg-HCO3	Yes
BGN-17	Bizana	Surface water	Mg-Ca-Cl-HCO3	No
BGN-2	Umzimkulwana River	Surface water	Na-Mg-HCO3	No
BGN-20	Bongwana	Groundwater	Na-Mg-Cl-HCO3	Yes

Station ID	Location	Sampling point	Water Type	CO_2-rich
BGN-21	Bongwana	Groundwater	Na-Ca-Mg-HCO3-Cl	No
BGN-22	Bongwana	Groundwater	Na-Ca-Mg-HCO3-Cl	No
BGN-3	Bongwana	Groundwater	Mg-Ca-Na-HCO3-Cl	No
BGN-4	Bongwana	Groundwater	Na-Mg-HCO3-Cl	No
BGN-6	Bongwana	Groundwater	Mg-Na-Ca-HCO3-Cl	No
BGN-7	Bongwana	Groundwater	Na-Mg-Ca-HCO3-Cl	No
BGN-8	Bongwana	Groundwater	Na-Mg-Ca-HCO3-Cl	No
BGN-9	Bongwana	Groundwater	Ca-Na-Mg-HCO3	No

5.3 Linkages among geochemical parameters of groundwater

Figure 5-4 to Figure 5-9 show correlations among the groundwater quality parameters from the study area. Ca^{2+} and Mg^{2+} are correlated with HCO_3^- for both travertine cones and boreholes. Ca^{2+} is further correlated with SO_4. Na is correlated with HCO_3, SO_4 and Cl. The correlations were done to determine the possible minerals that could have contributed in the reported concentrations of the elements correlated in the aqueous solution.

- ***Travertine cones springs***

The concentrations of Mg^{2+} and Ca^{2+} from the travertine cones display a good correlation with HCO_3 indicating that the weathering of Dolomite would be the possible rock that released the ions to groundwater. Good correlation is displayed between Ca^{2+} and SO_4 which may imply the dissolution of Gypsum and Anhydrite to groundwater. The concentration of Na was well correlated with both HCO_3 and SO_4^- indicating that the dissolution of Feldspar may have contributed to the observed concentration of sodium from travertine cone springs.

Based on the correlations, it is likely that the following chemical reactions might have occurred along the groundwater flow system from the recharge area to the discharge area:

$$CaMg(CO_3)_2\,(\text{Dolomite}) + 2CO_2 + 2H_2O \Leftrightarrow Ca^{2+} + Mg^{2+} + 4HCO^-_3. \quad (10)$$

$$CaSO_4\,(\text{Gypsum}) \Leftrightarrow Ca^{2+} + SO^{2-}_4. \quad (11)$$

$CaCO_3$ (Calcite) + CO_2 + H_2O ⇔ Ca^{2+} + $2HCO_3$. (12)

$2NaAlSi_3O_8 + 11H_2O + 2CO_2 \rightarrow Al_2Si2O5\ (OH)_4 + 2Na^+ + 2HCO_3^- + 4H4SiO_4$ (13)

- **Shallow boreholes**

Poor correlation between the concentration of Mg^{2+} and HCO_3 in the boreholes indicate that it is unlikely that the dolomite dissolution is responsible for the observed concentration of Mg^{2+} and HCO_3. However, good correlations between the concentration of Ca^{2+} and HCO_3^- and between Na^+ and Cl^- are observed. These correlations may imply that precipitation and shallow root zone processes dominant.

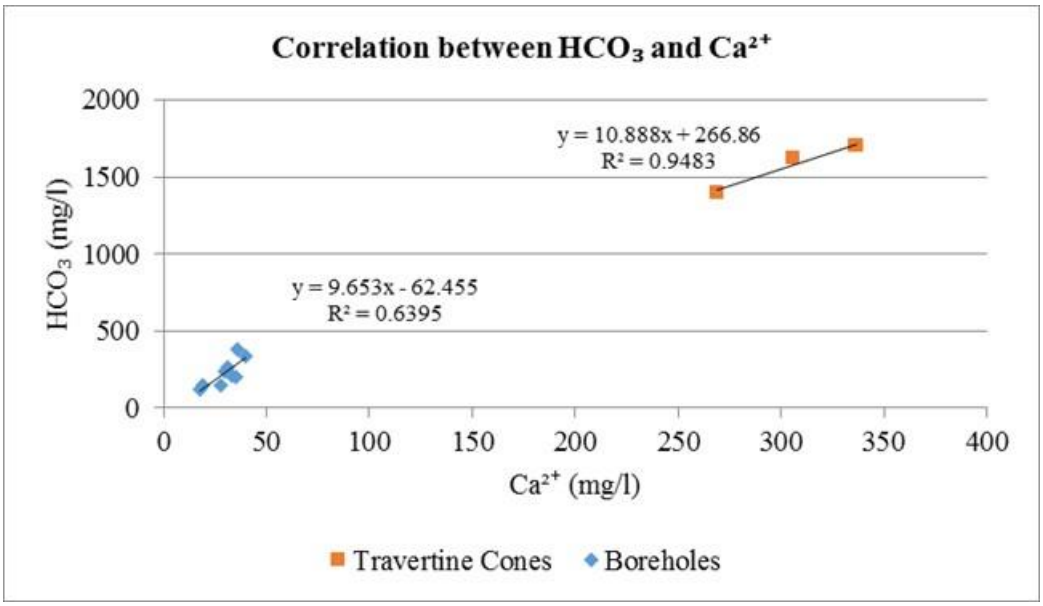

Figure 5-4: Correlation between HCO_3^- and Ca^{2+} in groundwater.

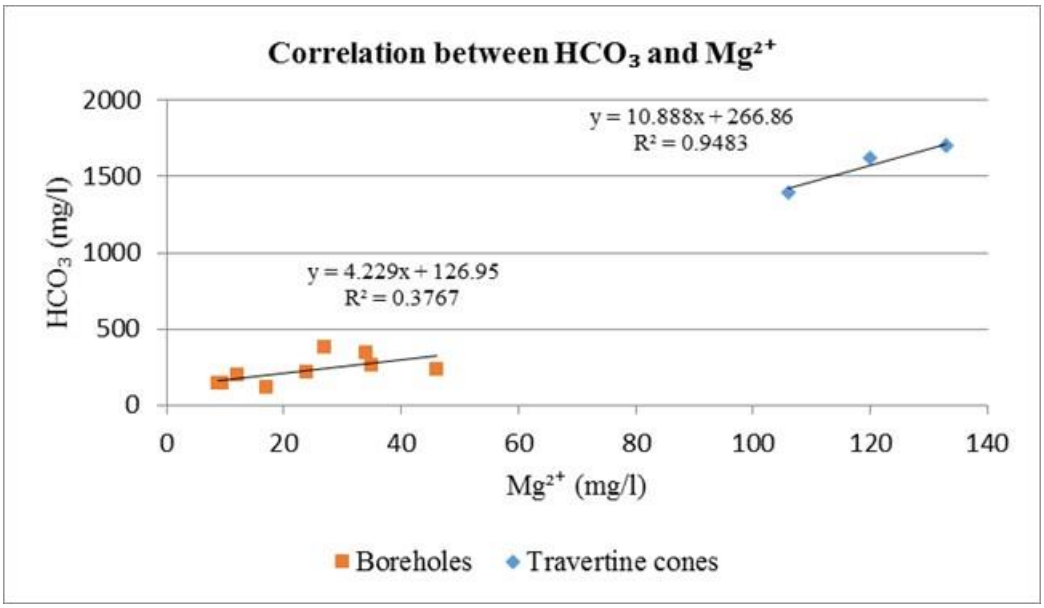

Figure 5-5: Correlation between HCO_3 and Mg^{2+} in groundwater.

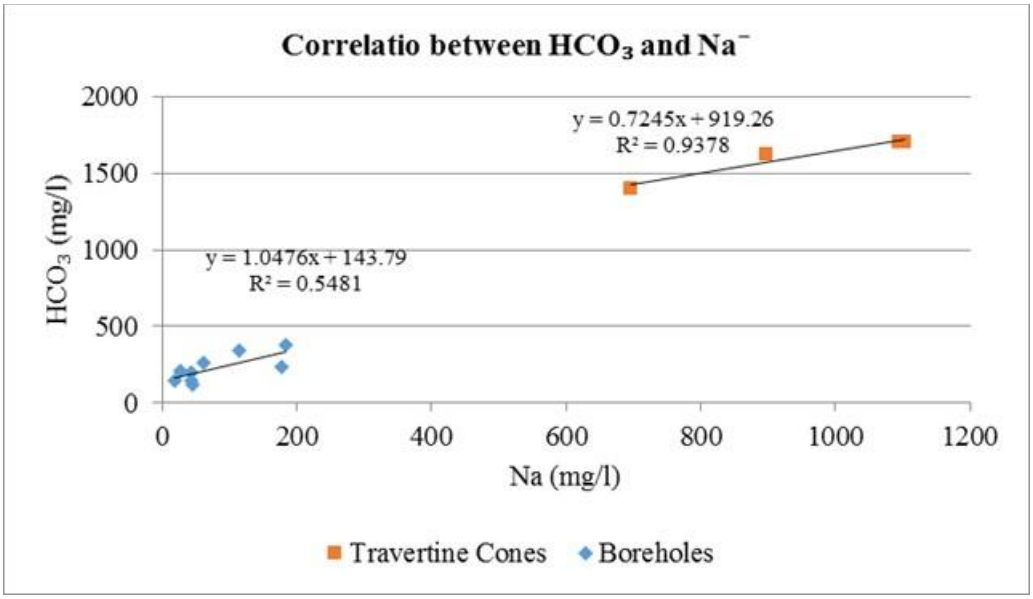

Figure 5-6: Correlation between HCO_3^- and Na^+ in groundwater.

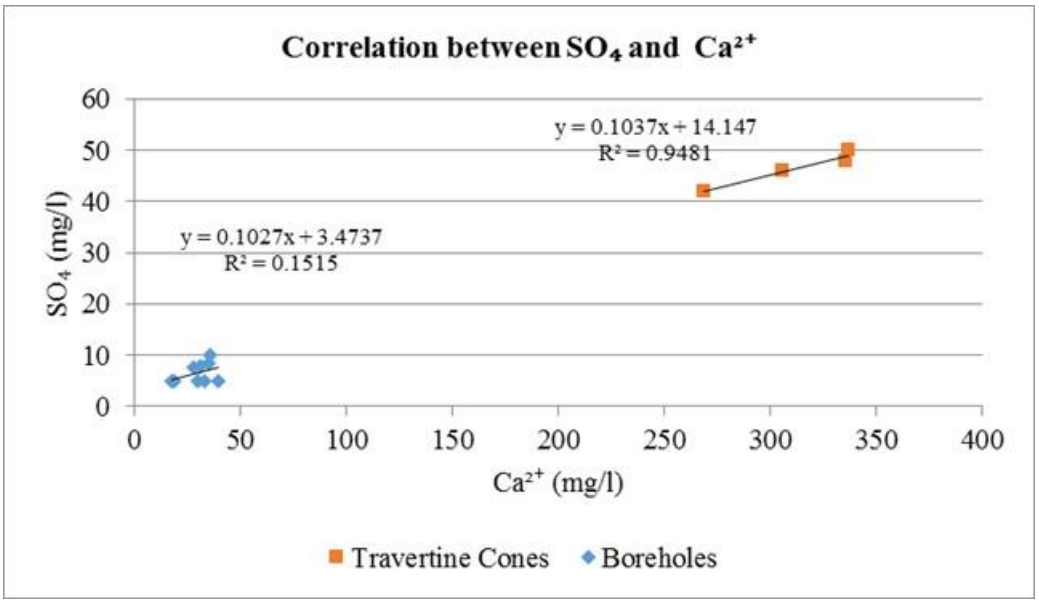

Figure 5-7: Correlation between SO_4^- and Ca^{2+} in groundwater.

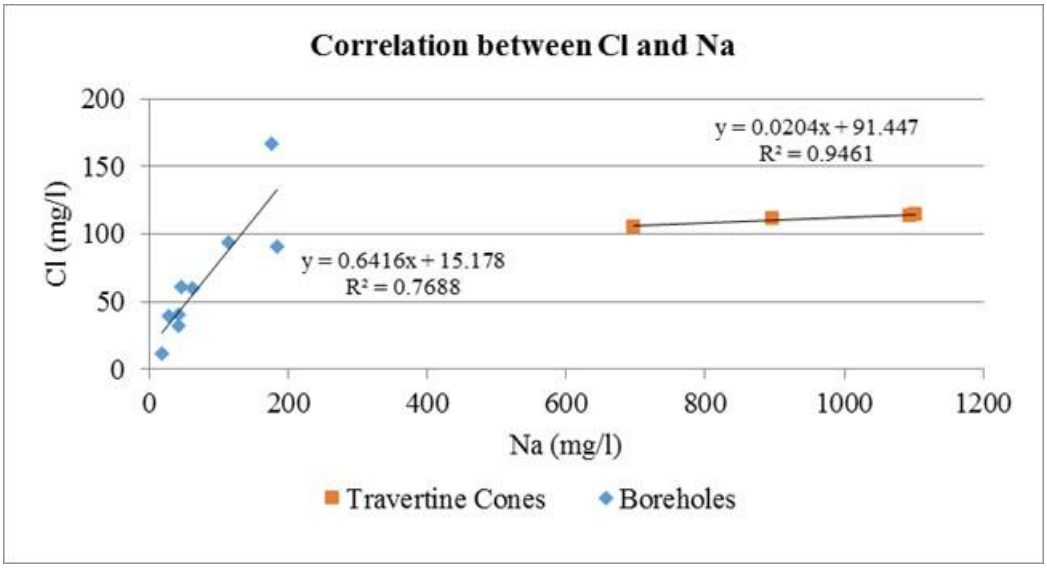

Figure 5-8: Correlation between Cl^- and Na^+ in groundwater.

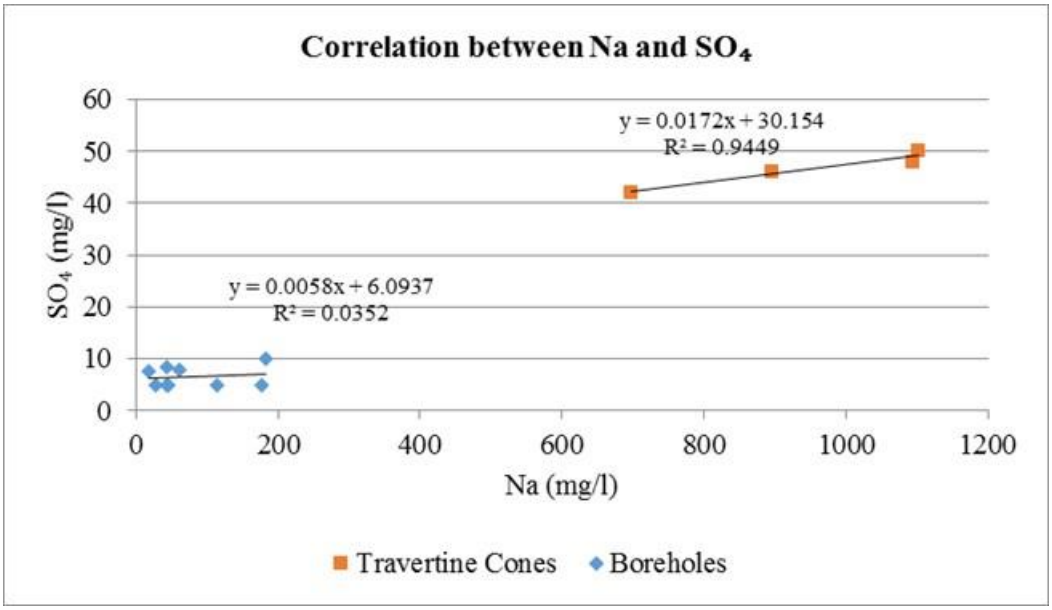

Figure 5-9: Correlation between SO_4^- and Na^+ in groundwater.

5.4 Saturation indexes of groundwater and surface water with respect to selected minerals

The chemical data was further modelled using the geochemical modelling code (Phreeqc) (Parkhurst and Appelo, 1999) to determine the saturation indices (SI) with respect to calcite, dolomite, gypsum, anhydrite and aragonite for all sampling points based on the following equation:

$$SI = \log [IAP/K_s] \quad (14)$$

Where IAP is the relevant ion activity product, which can be calculated by multiplying the ion activity coefficient i and the composition concentration mi, and Ks is the equilibrium constant of the reaction considered at the sample temperature. All these Phreeqc calculations assume a temperature of 25°C and pe value of 4. When the groundwater is at equilibrium with some minerals, SI equals zero; positive values of SI represent saturation or oversaturation, and negative values show under-saturation (Appelo and Postma, 1994; Drever, 1997). The calculated SI's for the minerals are presented in Table 5-4. Figure 5-10 shows a plot of saturation indices versus TDS for deep groundwater from travertine cone springs, shallow groundwater from boreholes and surface water from Umtamvuna and Umzimkulwana Rivers to show that these elements contributed to the elevated TDS values. The saturation indices for calcite,

dolomite and aragonite from travertine cone springs range from 0.74 to 0.82, 0.2 to 1.5 and -0.6 to 0.96, respectively. This indicates that water from travertine cone springs is oversaturated with respect to these carbonate minerals. However, the SIs of Anhydrite and gypsum for travertine cone springs appear to be negative, implying that these minerals are anticipated to dissolve or absent in the groundwater flow path. Shallow groundwater from the boreholes within the study area appear to be under-saturated (negative SIs) with respect to calcite, dolomite, anhydrite, gypsum and aragonite.

Table 5-4: Saturation indexes

Sample Type	Sample Name	SI Calcite	SI Dolomite	SI Anhydrite	SI Gypsum	SI Aragonite
Shallow groundwater from boreholes.	BGN3	-0.4036	-0.6247	-3.4329	-3.13	-0.55
	BGN4	-0.1428	-0.1061	-3.182	-2.88	-0.29
	BGN6	-0.3609	-0.3518	-3.3173	-3.01	-0.5
	BGN7	-0.1801	-0.1195	-3.4347	-3.13	-0.32
	BGN8	-0.9201	-1.534	-3.6604	-3.36	-1.06
	BGN20	-0.5939	-0.6707	-3.6085	-3.31	-0.74
	BGN21	-0.7163	-1.4422	-3.5942	-3.29	-0.86
	BGN22	-0.3584	-0.8636	-3.1459	-2.84	-0.5
	BGN9	-0.588	-1.3249	-3.2434	-2.94	-0.73
Deep groundwater from travertine cone springs.	BGN11	0.7415	1.3513	-2.0647	-1.76	0.6
	BGN12	0.7971	1.4806	-2.0212	-1.72	0.65
	BGN15	0.8192	0.2427	-3.8517	-3.55	0.96
	BGN16	0.8206	1.5255	-1.9834	-1.68	0.68
Surface water from rivers	BGN14	-1.4095	-2.5482	-3.6622	-3.36	-1.55
	BGN1	-0.8563	-1.5097	-3.6629	-3.36	-1
	BGN2	-0.8572	-1.5113	-3.6615	-3.36	-1

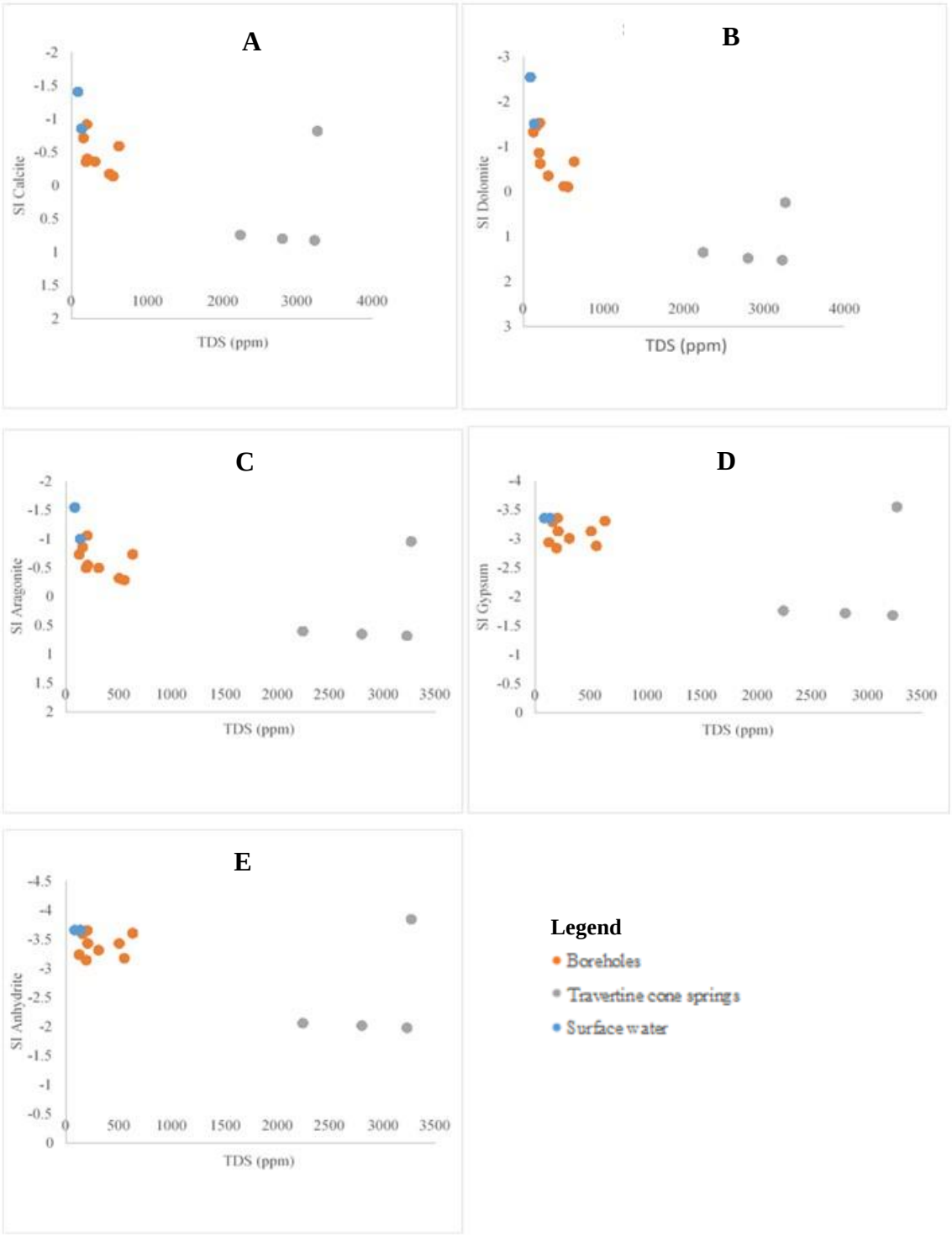

Figure 5-10: Plot of saturation indexes with respect to some minerals in water. A: plot of SI calcite vs TDS. B: Plot of SI dolomite vs TDS. C: Plot of SI Aragonite vs TDS. D: plot of SI Gypsum vs TDS. E: plot of SI anhydrite vs TDS.

5.5 Geochemical composition of travertine rock samples

Two thin sections were prepared from the travertine mound rock samples collected on either sides of Umtamvuna River. These samples were used to illustrate the petrographic and geochemical composition of the travertine deposits. The photos of the thin sections taken under microscope are shown in Figure 5-11. These thin sections show an extremely fine grained rock, consisting of calcite and few quartz fragments. The brown coloured materials are undifferentiated and possibly grew first and then followed by concretionary growth. The interspaces between concretionary growths is occupied with carbonates.

The geochemical composition of the travertine rocks samples are presented in Table 5-5. A ternary diagram of the oxide composition was constructed (Figure 5-12). Based the geochemical composition, the dominant oxide components of the travertine cones include CaO, SiO_2, Fe_2O_3, Al_2O_3 and MgO with average values of 46.23, 8.79, 6.335, 1.11 and 1.79 % respectively. Therefore, it can be seen that travertine composition is dominated by calcite followed by iron, aluminium and magnesium rich minerals.

The ICP-MS scan of the travertine cone trace element composition is presented in appendix C. Chromium, strontium, barium, zirconium, vanadium, cerium, lead, arsenic, rubidium and nickel are more abundant in concentration than other trace elements. The XRD results of the travertine cone rock samples indicate calcite and magnesium calcite mineralogy with minor silica (Figure 5-13 and Figure 5-14).

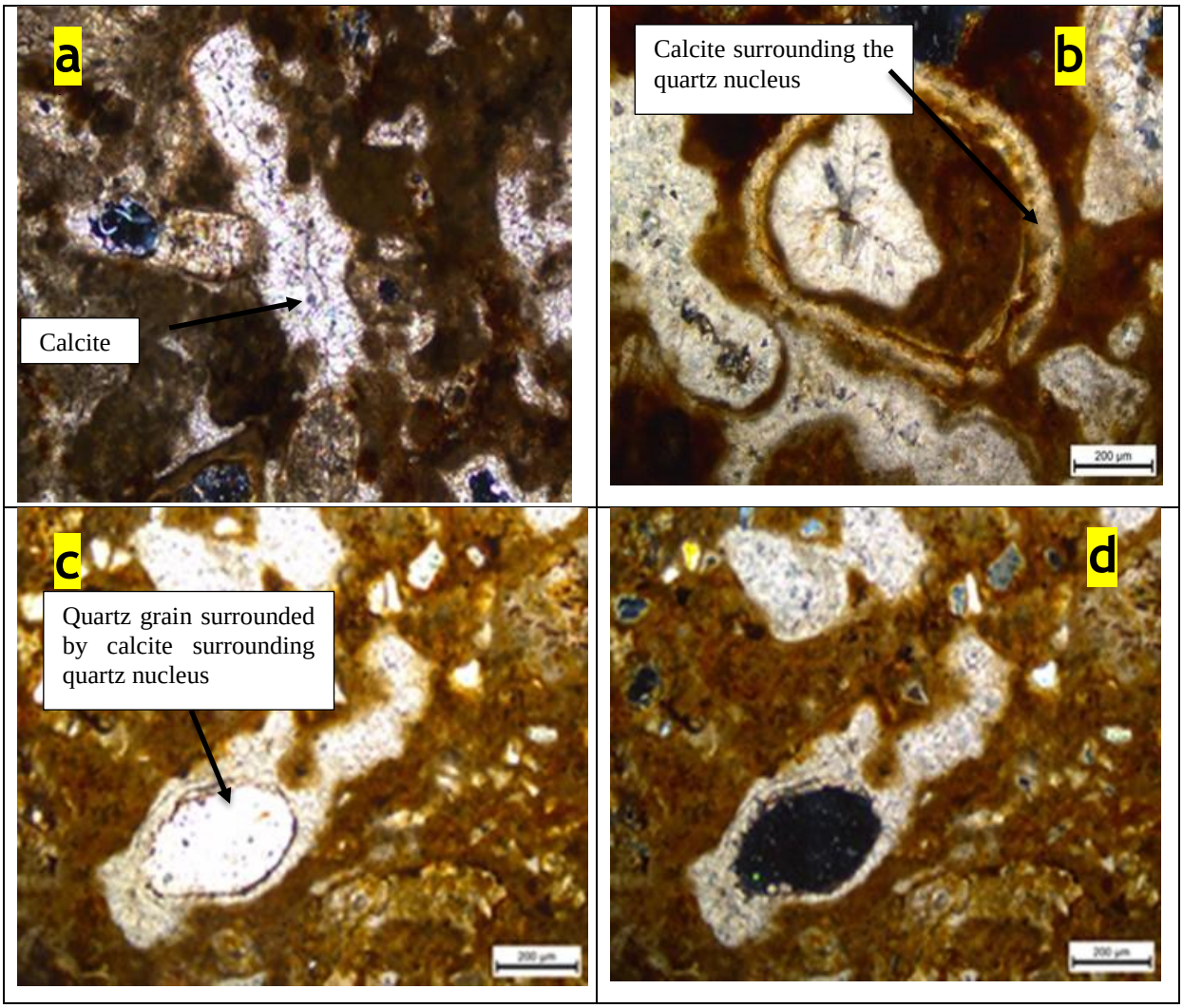

Figure 5-11: Thin section photos taken under polarised microscope.

Table 5-5: XRF analysis results of the travertine rock samples ML3 and ML4.

No.	Major oxides	Value (%)		
		Sample ML-3	**Sample ML-4**	**Average Value %)**
1	**Al_2O_3**	2.10	0.12	1.11
2	**CaO**	41.71	50.75	46.23
3	**Cr_2O_3**	bdl	bdl	bdl
4	**Fe_2O_3**	7.61	5.06	6.335
5	**K_2O**	0.32	0.02	0.17
6	**MgO**	1.74	1.84	1.79
7	**MnO**	0.34	0.40	0.37
8	**Na_2O**	0.28	0.06	0.17
9	**P_2O_5**	0.04	0.04	0.04
10	**SiO_2**	8.79	bdl	8.79
11	**TiO_2**	0.17	0.01	0.09
12	**L.O.I.**	36.45	42.51	
13	**Sum Of Conc.**	99.55	100.81	
Note that bdl (below detection limit) and L.O.I (loss on Ignition)				

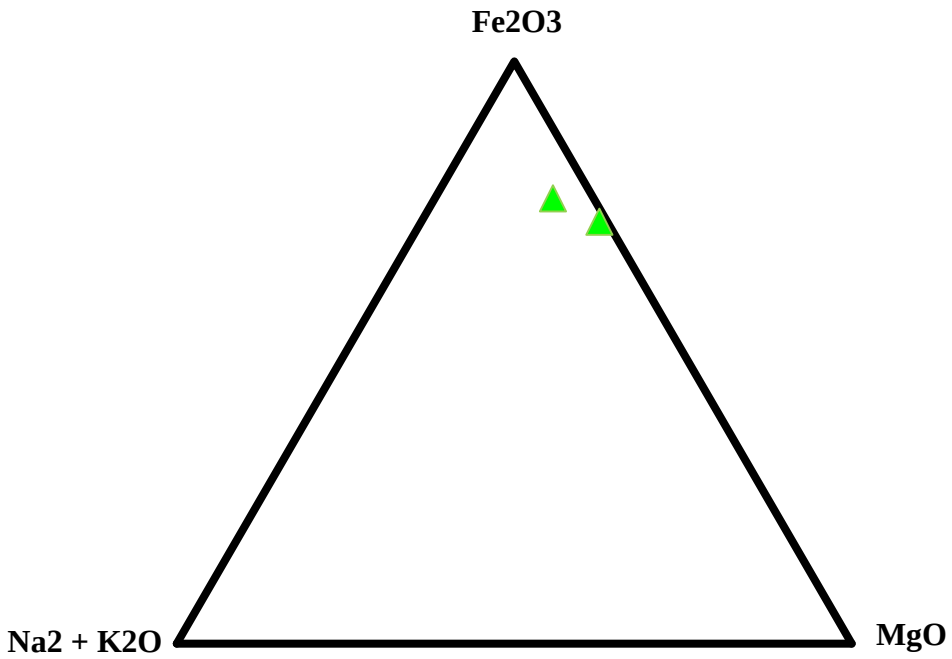

Figure 5-12: Ternary diagram of the travertine sample oxide composition (diagram drawn after Torres et al., (2000)).

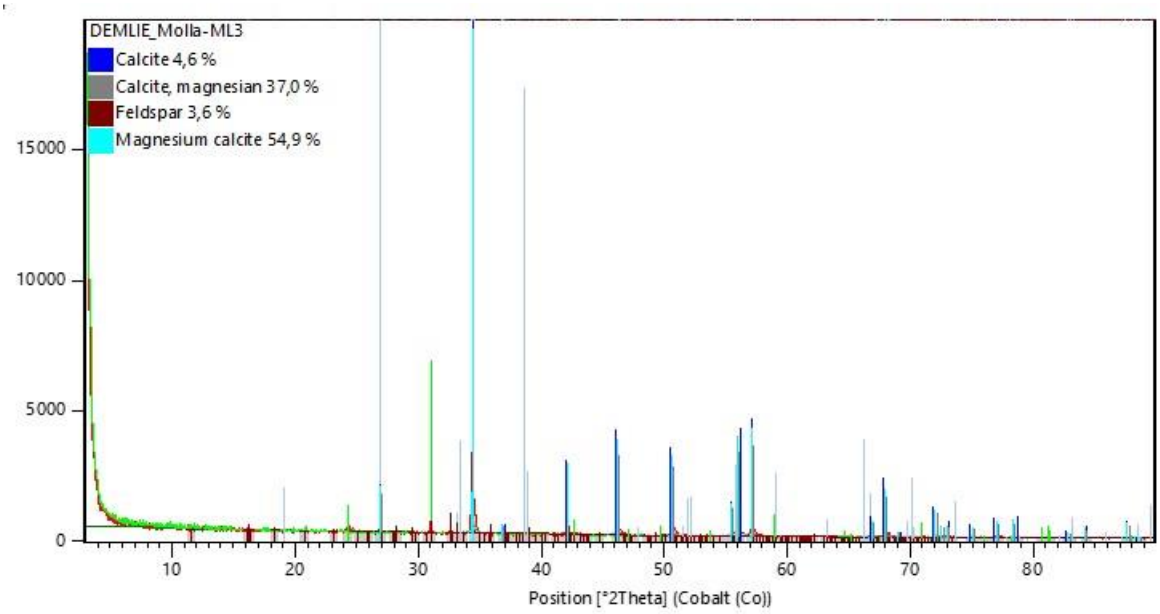

Figure 5-13: X-ray diffractogram of the travertine rock sample ML3.

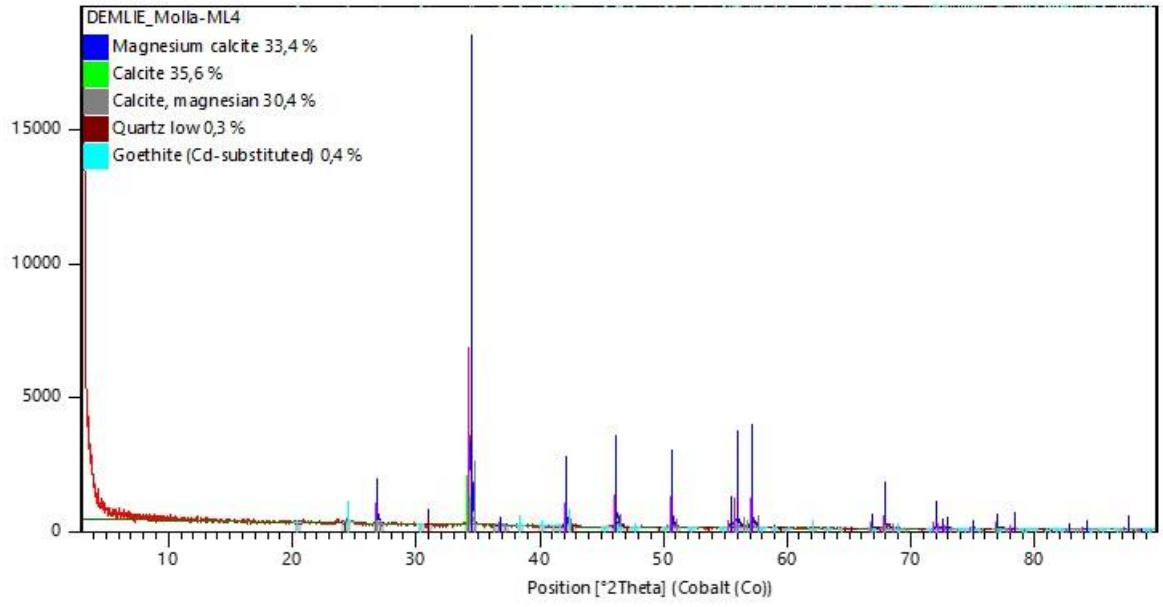

Figure 5-14: X-ray diffractogram of the travertine rock sample ML4.

5.6 Hydrogeochemical inverse modeling

Hydrogeochemical inverse modeling using Phreeqc was undertaken. The potential reactive phases for the inverse geochemical model were selected based on the hydrochemistry data, hydrogeochemical interpretations, XRF and XRD data of the travertine samples and saturation indices of water samples with respect to various minerals. Potential reactive minerals in the inverse modeling were constrained (precipitate/dissolve) following the conceptualization of the hydrogeology and hydrochemistry of the area. The inverse modeling takes into account uncertainty limits that are constrained to satisfy the mole balance for each element and valance state, as well as the charge balance for each solution within the simulation.

The simulations (sim) were constrained within the specified uncertainty limit, which were selected as 0.025 or 0.05 as default for all model runs. In the inverse model, the mineral phases such as calcite, dolomite, gypsum, anhydrite, aragonite, albite, K-feldspars, pyrite, and Flourite were set to dissolve and CO_2 is set to form. Other phases such as siderite, kaolinite, sylvite, and amorphous quartz were allowed to either dissolve or precipitation as they were required for the model to run.

The summary of the most optimum inverse model for the selected simulations with phase mole transfers for the minerals and gases along the flow paths are given in Table 5-8. Figure 5-15, Figure 5-16 and Figure 5-17 are the graphical representations of the inverse model results for the three travertine cone springs. The results of the inverse model shows that calcite, dolomite, K-feldspars, albite and fluorite are dissolving in groundwater and CO_2 is formed together with precipitation of amorphous silica, K-mica and siderite. The Ca^{2+} released by the dissolution of carbonate rocks leads to the precipitation of additional calcite, and an increase in CO_2, which leads to a slightly lower pH and supersaturation of calcite. Dissolution of sodium feldspars and albite are contributing the relatively high concentration of Na^+ in groundwater. The dissolution of pyrite, goethite and siderite is appears to be the main contributor of iron from the travertine springs.

Table 5-6: Inverse geochemical modelling for travertine springs

Mineral Phases	Phase state	Phase mole transfers Travertine Spring-1 (BGN-12)	Phase mole transfers active travertine cone spring (BGN-15)	Phase mole transfers active travertine mound spring (BGN-16)	Phase mole transfer Average
Calcite	dissolving	0.002940	0.002910	0.002940	0.002930
Dolomite	Dissolving	0.005480	0.005480	0.005480	0.005480
CO_2	Produced	-0.009990	-0.010120	-0.009990	-0.010033
Pyrite	Dissolving	0.000261	0.000250	0.000260	0.000257
Goethite	Dissolving	0.003880	0.003780	0.003880	0.003847
K-feldspars	Dissolving	0.020800	0.020640	0.020780	0.020740
Quartz	Precipitating	-0.138000	-0.136720	-0.137680	-0.137467
Siderite	Precipitating	-0.003910	-0.003750	-0.003910	-0.003857
Fluorite	Dissolving	0.000008	0.000010	0.000010	0.000009
Albite	Dissolving	0.048100	0.047720	0.048060	0.047960
Sylvite	Dissolving	0.003220	0.003190	0.003220	0.003210
kaolinite	Precipitating	-0.022900	-0.022790	-0.022950	-0.022880

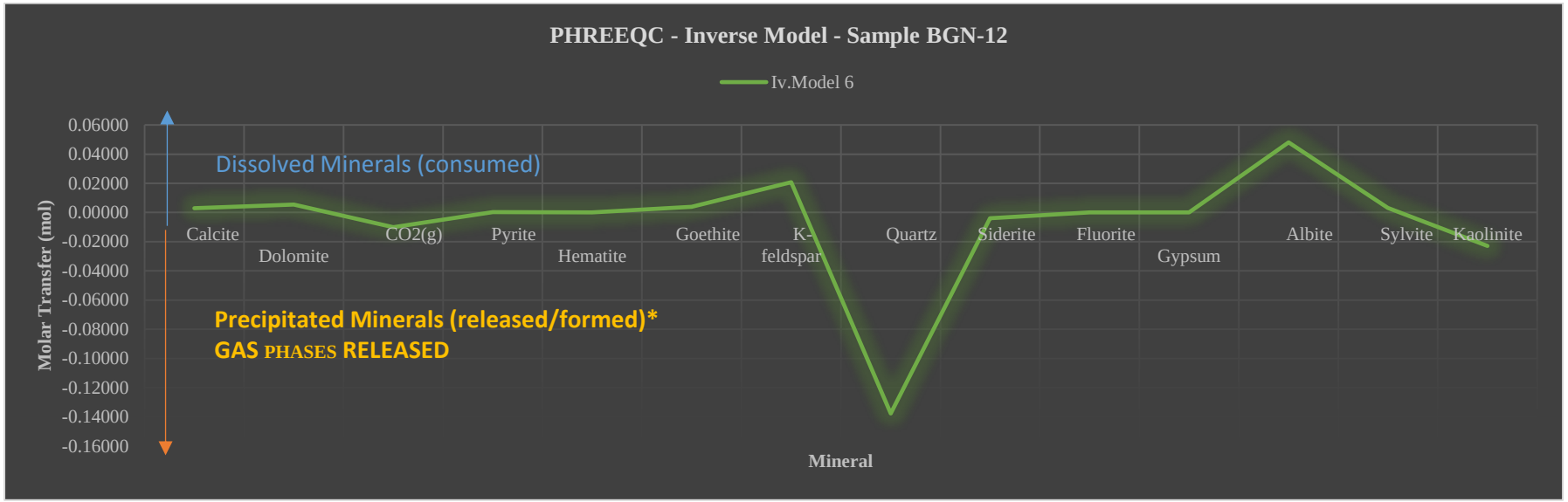

Figure 5-15: Graphical representation of the inverse model for travertine cone spring, sample number BGN-12.

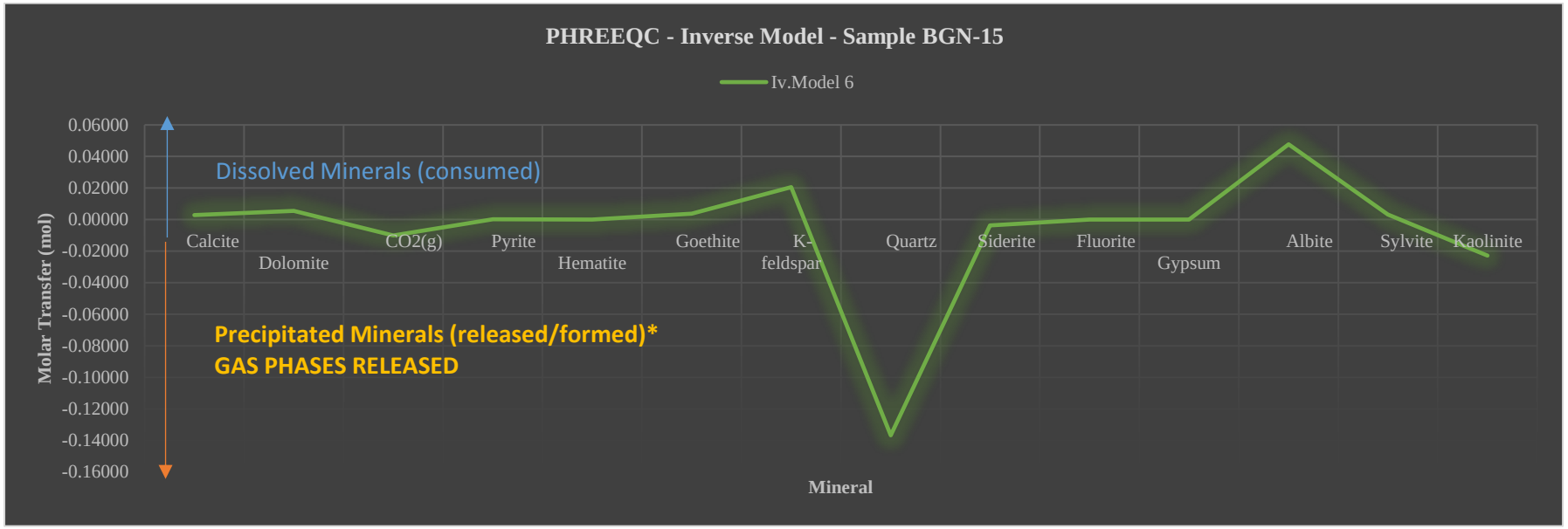

Figure 5-16: Graphical representation of the inverse model for travertine cone spring, sample number BGN-15.

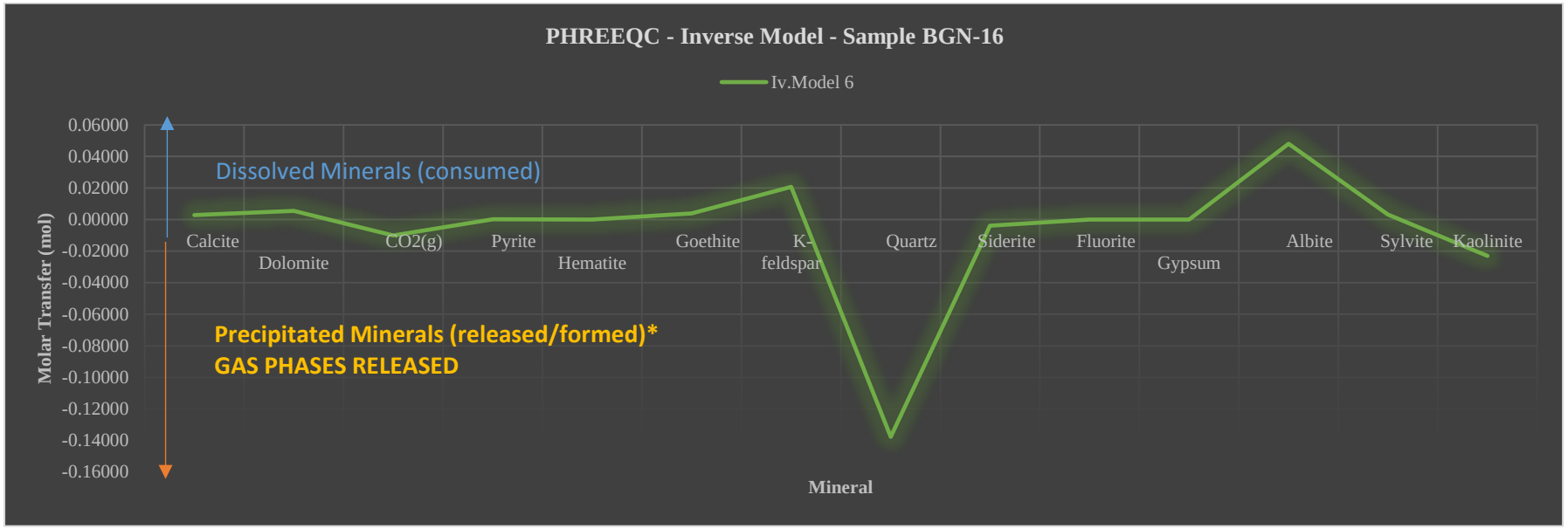

Figure 5-17: Graphical representation of the inverse model for travertine cone spring, sample number BGN-16.

5.7 Hydrogeochemical forward modeling

Forward modeling predicts the evolution of water composition based on hypothetical reactions, initial input information such as recharge composition. Forward modeling relies on a thermodynamic model of aqueous solutions and mineral phases to calculate solution composition. The objective of the forward geochemical modeling is to predict mineral solubilities, mass transfers, reaction paths, pH and pe by using available solid phase and aqueous data in aqueous specification models (Plummer, 1992).

In this study, forward modeling is combined with the results from the inverse modeling. The mole transfer results from inverse modeling determine the net mole transfer along the flow path, but these results are only based on the chemistry data at the end of the flow path. Therefore, forward modeling is used to prove thermodynamic consistency and validity for the mole transfer results of the inverse model, which implies that if the results of the inverse modeling are correct, the final composition from the forward model should be near or equal to the composition measured from the travertine cone springs for the selected hydrochemical parameters, such as Sodium, Calcium, pH, Iron, Magnesium, Fluorite, Potassium and Chloride). It is assumed that the springs originate from the same system and groundwater from all the springs flows along the same path. The average mole transfer from the three springs was used.

The results of the forward model show similar concentrations as those measured from the travertine springs for sodium, calcium, magnesium, potassium, iron, chloride and sulphate. This result supports the mole transfers obtained from the inverse model are consistent and valid. The graph of the forward model for the 50 steps is shown in Figure 5-18 and the results of the 50 steps are tabulated in Table 5-7.

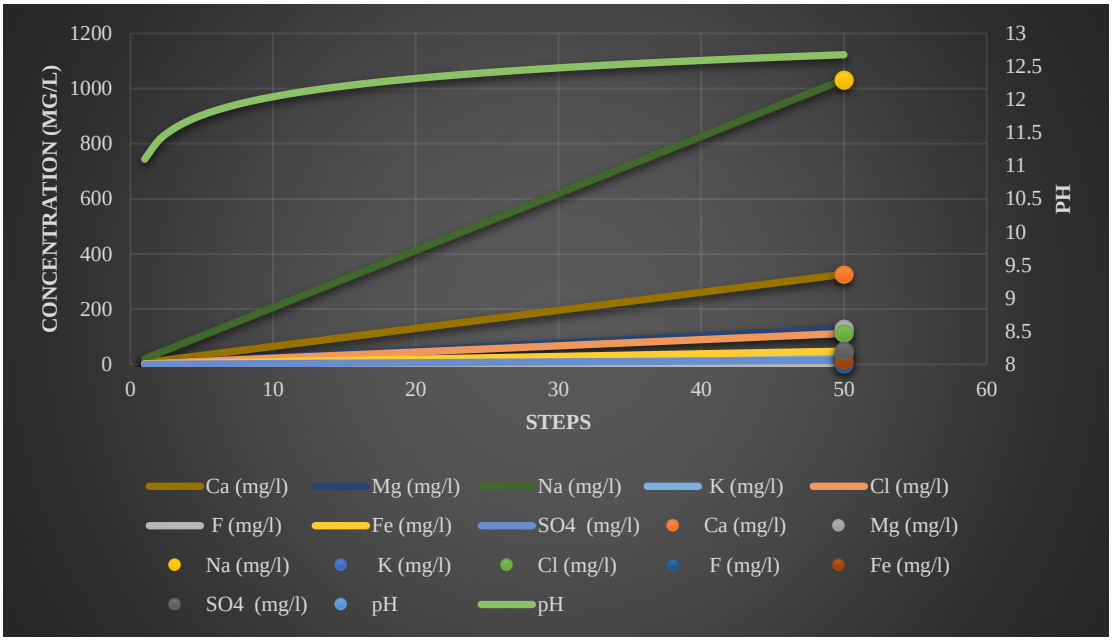

Figure 5-18: Forward model graph. The lines show the steps of the forward model and the dots at the end of the lines show the average concentration measured from the travertine springs.

Table 5-7: Forward model result for 50 steps.

sim	step	pH	Ca (mg/l)	Mg (mg/l)	Na (mg/l)	K (mg/l)	Cl (mg/l)	F (mg/l)	Fe (mg/l)	SO4 (mg/l)
1	1	11.0999	6.5312	2.5632	20.647	0.78142	2.2437	0.00621	0.96102	0.30453
1	2	11.3879	13.063	5.1264	41.294	1.5629	4.4874	0.01242	1.9221	0.60908
1	3	11.5548	19.594	7.6898	61.942	2.3444	6.7313	0.01862	2.8832	0.91364
1	4	11.6725	26.127	10.253	82.591	3.1259	8.9752	0.02483	3.8443	1.2182
1	5	11.7634	32.659	12.817	103.24	3.9074	11.219	0.03104	4.8055	1.5228
1	6	11.8375	39.191	15.381	123.89	4.689	13.463	0.03725	5.7667	1.8274
1	7	11.8998	45.724	17.944	144.54	5.4706	15.708	0.04346	6.7279	2.132
1	8	11.9537	52.257	20.508	165.2	6.2523	17.952	0.04967	7.6892	2.4366
1	9	12.0012	58.79	23.072	185.85	7.0339	20.196	0.05588	8.6506	2.7412
1	10	12.0435	65.324	25.636	206.5	7.8156	22.441	0.06209	9.6119	3.0459
1	11	12.0817	71.858	28.2	227.16	8.5974	24.685	0.0683	10.573	3.3505
1	12	12.1165	78.392	30.765	247.81	9.3791	26.93	0.07451	11.535	3.6552
1	13	12.1485	84.926	33.329	268.47	10.161	29.175	0.08072	12.496	3.9599
1	14	12.1781	91.461	35.894	289.13	10.943	31.42	0.08694	13.458	4.2646
1	15	12.2055	97.996	38.458	309.78	11.725	33.664	0.09315	14.419	4.5693
1	16	12.2312	104.53	41.023	330.44	12.507	35.909	0.09936	15.381	4.874
1	17	12.2553	111.07	43.588	351.1	13.288	38.155	0.10557	16.343	5.1787
1	18	12.2779	117.6	46.153	371.76	14.07	40.4	0.11178	17.304	5.4835
1	19	12.2993	124.14	48.718	392.42	14.852	42.645	0.118	18.266	5.7882
1	20	12.3196	130.67	51.283	413.09	15.634	44.89	0.12421	19.228	6.093
1	21	12.3389	137.21	53.848	433.75	16.416	47.136	0.13042	20.189	6.3978
1	22	12.3572	143.75	56.413	454.41	17.198	49.381	0.13664	21.151	6.7026
1	23	12.3748	150.28	58.979	475.08	17.981	51.627	0.14285	22.113	7.0074
1	24	12.3915	156.82	61.544	495.74	18.763	53.873	0.14906	23.075	7.3122
1	25	12.4076	163.36	64.11	516.41	19.545	56.119	0.15528	24.037	7.617
1	26	12.423	169.9	66.675	537.08	20.327	58.364	0.16149	24.999	7.9218
1	27	12.4378	176.43	69.241	557.74	21.109	60.61	0.16771	25.961	8.2267
1	28	12.4521	182.97	71.807	578.41	21.892	62.857	0.17392	26.923	8.5315
1	29	12.4658	189.51	74.373	599.08	22.674	65.103	0.18014	27.885	8.8364
1	30	12.4791	196.05	76.939	619.75	23.456	67.349	0.18635	28.847	9.1413
1	31	12.4919	202.59	79.505	640.42	24.239	69.595	0.19258	29.809	9.4462
1	32	12.5043	209.13	82.072	661.1	25.021	71.842	0.19879	30.772	9.7511
1	33	12.5164	215.67	84.638	681.77	25.803	74.088	0.205	31.734	10.056
1	34	12.528	222.21	87.205	702.44	26.586	76.335	0.21123	32.696	10.361
1	35	12.5393	228.75	89.771	723.12	27.368	78.582	0.21744	33.658	10.666
1	36	12.5503	235.29	92.338	743.79	28.151	80.828	0.22365	34.621	10.971
1	37	12.561	241.83	94.905	764.47	28.933	83.075	0.22987	35.583	11.276
1	38	12.5714	248.37	97.472	785.14	29.716	85.322	0.23608	36.546	11.581
1	39	12.5815	254.91	100.04	805.82	30.499	87.569	0.24231	37.508	11.886
1	40	12.5913	261.45	102.61	826.5	31.281	89.816	0.24852	38.471	12.191
1	41	12.6009	267.99	105.17	847.18	32.064	92.064	0.25475	39.433	12.496
1	42	12.6103	274.53	107.74	867.86	32.846	94.311	0.26096	40.396	12.801
1	43	12.6194	281.08	110.31	888.54	33.629	96.558	0.26719	41.358	13.106
1	44	12.6283	287.62	112.88	909.22	34.412	98.806	0.2734	42.321	13.411
1	45	12.637	294.16	115.44	929.91	35.195	101.05	0.27963	43.284	13.716
1	46	12.6456	300.7	118.01	950.59	35.978	103.3	0.28584	44.246	14.021
1	47	12.6539	307.25	120.58	971.27	36.76	105.55	0.29207	45.209	14.326
1	48	12.662	313.79	123.15	991.96	37.543	107.8	0.29828	46.172	14.631
1	49	12.67	320.34	125.71	1012.6	38.326	110.04	0.3045	47.135	14.936
1	50	12.6778	326.88	128.28	1033.3	39.109	112.29	0.31071	48.098	15.242
Phase mole transfer average	50	6.67	326.3	128.6	1031.6	39	112.6	0.31	15.2	48

5.8 Environmental isotope signatures

The analysis of the stable isotopes ($\delta^{18}O$ and $\delta^{2}H$) were carried out for shallow groundwater, surface water and travertine cone springs samples collected from the study area. The results are presented in Table 5-8 and plotted in Figure 5-19. The composition of the stable isotopes for shallow groundwater appears to constitute depleted heavy isotope values with small variations amongst all the boreholes. However, it is evident that CO_2-rich groundwater from travertine springs and CO_2-rich borehole are much more depleted with respect the heavy isotopes compared to CO_2-free groundwater. It is a common phenomenon that the presence of CO_2 in groundwater systems changes the composition of oxygen isotope (Karolyte, 2017). This could happen either by promoting low temperature primary mineral dissolution and secondary mineral precipitation reactions, preferentially removing the heavy isotopes or by equilibrium oxygen isotope exchange between CO_2 and groundwater. Both of these processes affect only the oxygen isotope values while hydrogen isotope values remain unchanged, unless water-rock reactions involve extensive precipitation of hydrogen-rich clays (D'Amore and Panichi, 1987). In the case of groundwater from the travertine springs and the CO_2-rich borehole, it can be seen that both hydrogen and oxygen isotope composition have shifted towards the lighter or depleted isotopic signal (Figure 5-19). As a result, groundwater from the travertine springs displays a horizontal departure from the MWL, typical of CO_2-rich water, to the left indicating low temperature mineral reactions.

Tritium composition of groundwater determined mainly to deduce the age of groundwater, because groundwater tritium concentrations reflect precipitation tritium levels during recharge. Groundwater age estimation using tritium only provides semi-quantitative, “ball park” values. Low tritium concentrations were detected from the travertine cone springs, shallow groundwater boreholes and rivers. The deep circulating groundwater from travertine cone springs is sub-modern in age and shallow circulating groundwater from boreholes and surface water from rivers comprise a mixture of sub-modern and modern aged waters.

Table 5-8: Results of stable isotope analysis for the various water samples

Sample Name	Sample type	δ^2H (‰)	$\delta^{18}O$ (‰)	d-excess (‰)	^3H (TU)
BGN-1	Umzimkulwana River	10.4	0.89	3.28	1.7
BGN-19	Umtamvuna River	-2.4	-1.61	10.48	2.8
BGN-14	Umtamvuna River	3	-0.82	9.56	1.2
BGN-3	Shallow groundwater borehole	-10.1	-3.42	17.26	0.7
BGN-4	Shallow groundwater borehole	-16	-3.95	15.6	1.0
BGN-6	Shallow groundwater borehole	-11.6	-3.39	15.52	1.4
BGN-7	Shallow groundwater borehole	-10.9	-3.7	18.7	0.7
BGN-8	Shallow groundwater borehole	-13.3	-3.92	18.06	1.0
BGN-9	Shallow groundwater borehole	-10.3	-3.5	17.7	3.0
BGN-10	Shallow groundwater borehole	-8.6	-3.5	19.4	0.6
BGN-21	Shallow groundwater borehole	-10	-3.17	15.36	1.0
BGN-22	Shallow groundwater borehole	-8.3	-2.81	14.18	0.4
BGN-17	Spring	-13.6	-3.65	15.6	1.2
BGN-18	Spring	-11.4	-3.09	13.32	0.3
BGN-20	CO_2-rich borehole	-18	-4	14	1.6
BGN-11	Travertine-N	-18.1	-6.52	34.06	0.4
BGN-12	Spring-N	-17.9	-6.95	37.7	0.0
BGN-15	Travertine-E1	-20.4	-7.78	41.84	0.9
BGN-16	Travertine-E2	-21.5	-7.23	36.34	1.1

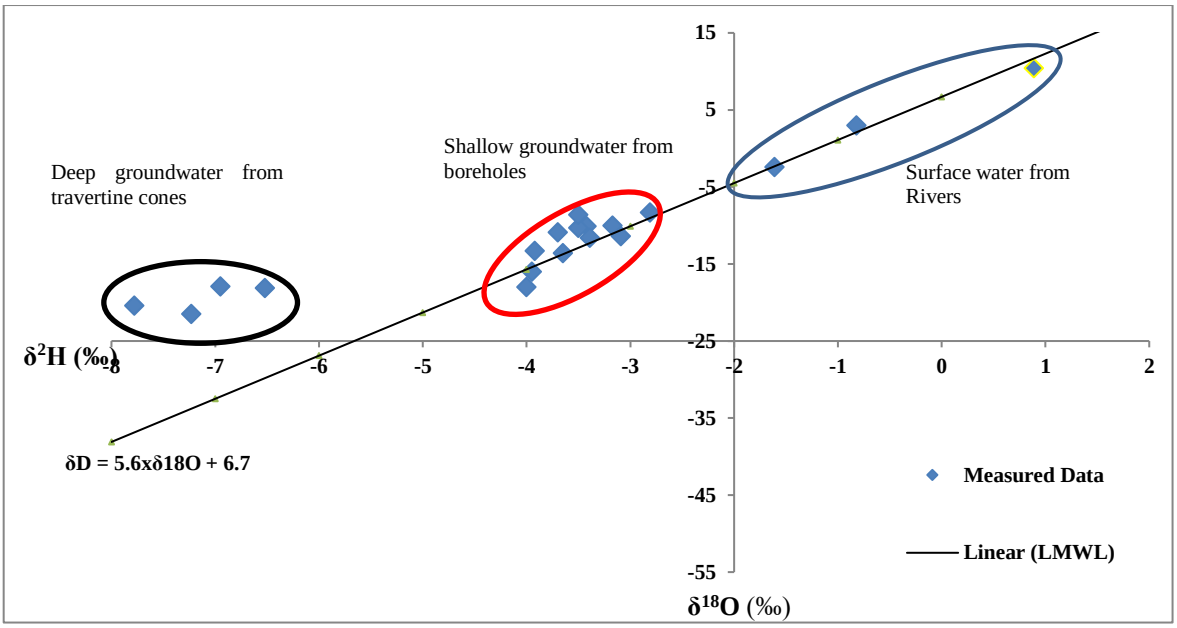

Figure 5-19: Relationship between oxygen and hydrogen isotopes in shallow groundwater, surface water and travertine cone springs in the study area. Local Meteoric Water Line (LMWL) is shown for comparison.

6. CHAPTER 6: DISCUSSION

6.1 CO_2 impacts on groundwater and surface water

Field measurements of EC, TDS, pH and hydrochemical analysis of major ions of groundwater and surface water from the study area (CO_2-rich and CO_2-poor sites) confirms that low pH, elevated TDS and EC values measured from the CO_2-rich sites are the result of dissolved CO_2 in groundwater. The ambient groundwater quality at these CO_2-rich sites has been altered by the introduction of CO_2 resulting in elevated concentration of major ions compared to CO_2-free sites. CO_2-free sites display neutral to slightly alkaline pH, low EC and TDS and low ionic concentrations. Therefore, the impacts of CO_2 on groundwater in the Bongwana area appear to be limited to CO_2-rich sites. The CO_2 migration along the fault appears to be limited to permeable zones due to fracturing and groundwater along these relatively high permeability zone along the fault is most likely to be impacted as well. However, groundwater that is hosted in the shallow aquifer that is not connected to the fault zones appears to be not impacted by CO_2. It is further noted that the impacts are minimal in surface water compared to groundwater resources. This could be due to loss of CO_2 to the atmosphere at the surface of the emission point and dilution effects resulting in low amounts of CO_2 dissolving in rivers compared to groundwater.

6.2 Evolution of groundwater hydrochemistry

Mineral dissolution at low temperatures due to dissolved CO_2 appears to be the main factor controlling the evolution of groundwater chemistry of the travertine springs and the CO_2-rich borehole along the fault zone. The correlation among groundwater parameters for the travertine cone springs suggest the dissolution of carbonate minerals (calcite, dolomite, aragonite, gypsum and anhydrite) and feldspars leading to elevated TDS values. Groundwater from travertine springs displayed positive SIs with respect to calcite, dolomite and aragonite indicating that the springs are oversaturated with respect to these carbonate minerals.

The oversaturation of groundwater from these springs with carbonates is also displayed by the deposition of the travertine mounds. The deposition of such quantities of carbonates from the springs can only be explained by the existence of a large carbonate source at depth below the site as it is unlikely that such volumes of carbonates could have come from the Dwyka Group sediments. The known carbonate rocks in the area belong to the Marble Delta Formation which outcrops approximately 30-40km northeast of the Bongwana fault and are commercially exploited for high grade calcite and dolomite cement production. It could be possible that the same rocks occur below the Bongwana fault, underlying the Dwyka Group rocks and are responsible for the supply of carbonate minerals into groundwater.

6.3 Origin of CO_2

Assuming that the carbonate rocks exist at depth below the study area, the water percolating through the overlying pyritic carbonaceous shales of the Ecca Group and the Dwyka Group sediments leaches pyrite from these sediments. These leaching forms sulfuric acid through the reaction between pyrite and oxygen rich groundwater. The chemical reaction that represents the chemistry of pyrite weathering to form sulphuric acid in groundwater is given by equation 15 as:

$$2FeS_2 + 7O_2 + 2H_2O \rightarrow 2FeSO_4 + 2H_2SO_4 \quad (15)$$

This reaction generates two moles of acidity for two moles of pyrite oxidized. Ferrous iron is converted to ferric iron by the following reaction.

$$2\ FeS_2 + 7\ O_2 + 2\ H_2O \Rightarrow 2\ Fe^{2+} + 4\ SO_4^{2-} + 4\ H^+ \quad (16)$$

Another reaction which may occur is the hydrolysis of iron. Three moles of acidity are generated as a by-product.

$$4\ Fe^{2+} + O_2 + 4\ H^+ \Rightarrow 4\ Fe_{3+} + 2\ H_2O \quad (17)$$

The ferric iron generated in the above reaction may further oxidise additional pyrite.

$$FeS_2 + 14\ Fe^{3+} + 8\ H_2O \Rightarrow 15\ Fe^{2+} + 2\ SO_4^{2-} + 16\ H^+ \quad (18)$$

This is the cyclic and self-propagating part of the overall reaction and takes place very rapidly and continues until either ferric iron or pyrite is depleted. Note that in this reaction, iron is the oxidizing agent, not oxygen.

The acidic conditions in groundwater generated by the weathering of pyrite triggers the dissolution of carbonate rocks to produce CO_2 according to the following reactions.

$$CaCO_3\ (s) + H_2SO_4\ (_{aq)} => CaSO_4 + H_2O + CO_2\ _{(g)}\ (\text{Calcite}) \quad (19)$$

$$MgCO_3 + H_2SO_4\ _{(aq)} => MgSO_4 + H_2O + CO_2\ _{(g)}\ (\text{Dolomite}) \quad (20)$$

Once the CO_2 gas is produced it will dissolve in groundwater and produce more hydrogen ions that will further dissolve more carbonate rocks and produce more CO_2 following the model proposed by Gevers (1941) which suggests that the CO_2 generation is by the reaction of carbonate rocks at depth with acidic groundwater. The carbonated groundwater with dissolved CO_2 rises through the permeable fault zones and fractures to the earth surface.

6.4 Origin and age of groundwater.

The correlation among geochemical parameters of groundwater display a significant difference between groundwater from the boreholes within the Bongwana area and groundwater from the travertine cone springs near Umtamvuna River. The difference is also clearly shown by the stable isotope composition of the water samples. The stable isotopic composition for boreholes reflects local and modern meteoric recharge while the stable isotopic composition for travertine cone springs indicates a negative shift from the LMWL. These observations indicate that the reservoir and source of recharge for the deep circulating groundwater are different from the shallow groundwater or stable isotope exchange reaction has taken place. The reason for the negative shift from the LMWL of the travertine cone spring waters could be attributed to either consumption of oxygen isotope due to the dissolution of primary minerals and the precipitation of the secondary minerals at low temperatures or the exsolution of CO_2 at low temperature as the carbonated waters rises to the earth surface. The exsolution of moderate amounts of CO_2 at low temperature near the earth surface is known to lower the concentration of $\delta^{18}O$ in water (Ian et al., 2002).

The exsolution of CO_2 is even more significant in carbonated waters and reduction of $\delta^{18}O$ values is higher. Mixing of deep circulating groundwater and shallow circulating groundwater is evident from the study area and is displayed by the tritium results. Shallow groundwater from boreholes in the study area constitute waters that range between modern and sub-modern in age with the majority showing mixture between modern and sub-modern. Travertine springs groundwater display sub-modern age waters with the exception of BGN-16 which shows mixture between sub-modern and modern ages.

6.5 Implication for CCS in South Africa and the need for robust monitoring.

South Africa is a water scarce country and has recently been experiencing severe drought conditions in most parts of the country. The proposed area for the pilot CCS activities in South Africa underlies the major primary aquifer in the country that source for water supply to many people and the ecology. The environmental concern with the CO_2 injection into subsurface geological formations is the unintended leakage into fresh water resources. At low concentrations, the impact of CO_2 is limited, however, if the concentration increases it may be detrimental to environmental processes and functions. Vertical migration of leaking CO_2 will be accompanied by dissolution into shallow aquifer. Dissolved CO_2 hydrolyzes to form carbonic acid, which can alter pH. Since pH is a master variable in water-mediated chemical and biological reactions, a pH shift may cause undesirable changes in hydrochemistry, water quality, and ecosystem health. Examples include mobilization of toxic heavy metals and leaching of aquifer minerals. Therefore, any CO_2 leakage into fresh groundwater and surface water resources may have severe implications on potable and environmental water quality. However, the risk can be reduced if all scientific site selection protocols are adhered to and proper early detection systems are put in place. Furthermore, comprehensive rules and regulations for CCS operations should be in place prior to any licensing as well as a comprehensive groundwater monitoring plan.

6.7 Lessons learnt from the Bongwana study

The Bongwana groundwater study presents a good analogue to study and monitor the impacts of CO_2 leakage from a failed underground CO_2 storage facility. The technique and methodology required for CO_2 leakage detection and groundwater monitoring requires a better understanding of the leakage mechanism as well as changes in hydrochemical composition of groundwater and surface water due to interaction with CO_2 leaking from a sequestration facility. This research presents the groundwater parameters that are indicative of CO_2 interaction with fresh water resources based on the analysis of the Bongwana monitoring project.

The results of the field measurements and hydrochemical information obtained from the Bongwana study demonstrate clear impacts of natural CO_2 on groundwater and surface water quality. The CO_2-rich groundwater and surface water displayed elevated concentrations of dissolved chemical components which are of concern to drinking water quality. TDS and EC values as well as sodium and iron concentrations exceeded the SANS 241:2015 drinking water quality limits. Water from these sites may not be used for drinking purposes due to the potential health risks. Therefore, leakage of CO_2 into freshwater aquifers and surface water bodies has potential risks to water resources quality.

6.8 Shallow groundwater monitoring system

CO_2 leakage detection in the overlying potable aquifers at a CCS site requires precise and sensitive geochemical parameters that can be used for monitoring the presence of CO_2 in groundwater (Yang et al., 2014). Field measurements such as pH, EC, TDS, DO, salinity, Eh and DIC are considered some of the most important approaches for assessing responses of geochemical parameters to CO_2 leakage for leakage detection in groundwater. In addition to the field measurements, the analysis of the changes in ambient groundwater quality near the sequestration site in also important. Sudden changes in groundwater quality may be indicative of dissolved CO_2.

Field monitoring, measurements and hydrochemical analysis to detect CO_2 leakage are factors that could mitigate the impact of CO_2 leakage on shallow groundwater quality. However, CO_2 leakage is difficult or impossible to detect, because of the fact that simple mixing and dilution of CO_2-impacted groundwater with ambient groundwater, pH buffering reactions such as calcite dissolution and/or silicate mineral weathering, limited trace metal availability in aquifer minerals, and trace metal scavenging by secondary mineral precipitation interfere with the monitored information. Therefore, it is important to understand these processes and factors around the sequestration site before commencing with groundwater monitoring.

6.9 Hydrogeological conceptualization of the occurrence and circulation of shallow groundwater and deep CO_2-rich groundwater along the Bongwana Fault

Figure 6-1 shows a conceptualization of the hydrogeology of the study site indicating areas of high rainfall recharge and inferred groundwater flow around the Bongwana fault zone. Blue arrows denote rainfall recharge and black arrows denote groundwater flow directions. Precipitation in the study area increases with altitude, generally from east to west. High groundwater recharge rate occurs to the west the of the Bongwana fault. Shallow groundwater circulation is recharged by direct precipitation and potentially from losing rivers. Deep groundwater circulation is recharged from shallow groundwater that percolates to greater depths through deep fractures and faults. It is also possible that deep circulating groundwater is recharged through the Bongwana fault itself, especially from the mountainous areas to the west. Since the Dwyka Group rocks are characterized by massive tillites, deep circulating groundwater is potentially recharged at a greater distance from the study area. Percolating groundwater is acidified through leaching of pyrite within the Ecca Group. At depth, acidic groundwater reacts with carbonate rocks to produce CO_2. Deep groundwater flow and CO_2 migration occurs at depth following the preferential groundwater flow paths such as fractures, and faults. Since the CO_2 springs and the travertine cone springs are associated with the Bongwana fault, it is assumed that deep carbonated groundwater flow along the Bongwana fault zone. The travertine cone springs are at the lowest topography along the Bongwana fault and this may imply that the flow of groundwater is from high to low topography or vertical upward due to prevailing hydraulic gradient.

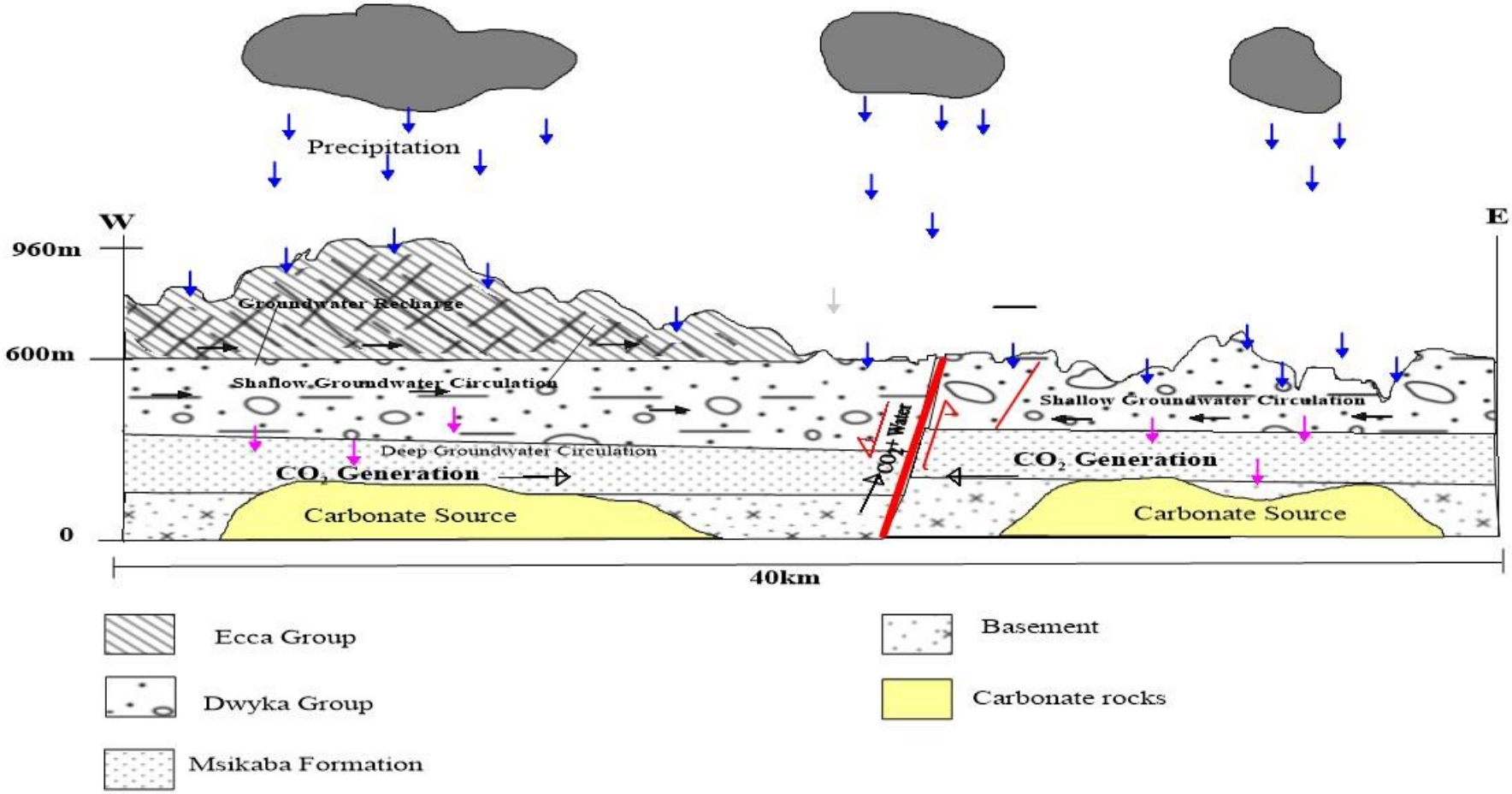

Figure 6-1: Conceptual diagram indicating groundwater recharge and inferred flow direction.

7. CHAPTER 7: CONCLUSIONS AND RECOMMENDATIONS

7.1 Conclusions

Characterisation of the CO_2 springs associated with the Bongwana fault and the assessment of their impacts on groundwater and surface water quality have been undertaken. The combination of onsite field measurements, hydrochemistry and isotopic composition of groundwater and surface water in the study area have provided a better understanding of the origin of groundwater and the processes that control the evolution of groundwater chemistry in the area. Furthermore, the field measurements and hydrochemical results have displayed clear impacts of the CO_2 springs on groundwater and surface water chemistry within the emission sites. The pH, EC and TDS measurements from CO_2-rich sites indicated low pH and elevated EC and TDS values compared to CO_2-free sites. The hydrochemical composition of groundwater from CO_2-rich sites is dominated by elevated Na^+, K^+, Mn, Fe, Ca^{2+} and HCO_3^- concentrations compared to groundwater and surface water from CO_2-poor sites. Groundwater from the travertine cone springs can be separated from the shallow groundwater from the boreholes in the Bongwana area on the basis of their isotopic composition. Shallow groundwater is of local and modern meteoric origin. The isotopic composition of travertine cone springs show a negative shift from the LMWL which is typical for CO_2-rich groundwater.

The correlation analysis of major ions in groundwater and the calculation of saturation indices have indicated that the dissolution/weathering of carbonate minerals (calcite and dolomite) have contributed to the hydrochemistry of groundwater from travertine cone springs. Major ions piper plot show that the chemical property of groundwater from travertine cone springs is dominated by Na-Ca-Mg-HCO_3 hydrochemical types or facies, while shallow groundwater from boreholes show Ca-Na-Mg-HCO_3 hydrochemical facies. Based on all available data, the most plausible model for the origin of CO_2 in the Bongwana area is the reaction of acidic groundwater with carbonate rocks at depth which was initially proposed by Gevers (1941). The evidence of the existence of the carbonate rock as a source of carbonate minerals (calcite and dolomite) is displayed by the large deposition of travertine mounds as well as oversaturation of from travertine cone springs with respect to calcite and dolomite.

Furthermore, the results of the inverse geochemical modelling for the travertine cone springs indicate that the mineral phases contributing to the overall chemistry of the springs are mainly carbonate minerals. Although the Dwyka Group sediments contain some carbonate minerals that could possibly affect groundwater chemistry, it is possible that carbonate rocks at depth account for the volume of carbonate minerals dissolved in groundwater and formation of travertine mounds on surface.

The Bongwana fault and the associated CO_2 springs present an excellent analogue to understand the impacts of CO_2 leakage due to injection well failure or leakage from an abandoned well or gradual leakage through undetected fault, fractures or wells from a failed CO_2 storage site. The findings of this study provide a clear picture of the impacts the CO_2 on groundwater and surface water resources. It is worth mentioning that South Africa is currently experiencing water shortages due to prolonged drought conditions in most parts of the country. The impact will be severe should any undetected CO_2 leakage from the storage site occurs into fresh water resources. However, it is believed that strict scientific site selection protocols and CO_2 leakage detections monitoring systems, together with proper remedial plans in place, will most likely minimise the risk of CO_2 leakage from a subsurface sequestration facility.

7.2 Recommendations

The current monitoring network for the Bongwana project comprise a limited number of groundwater boreholes that are located in vicinity of the emission sites. The data obtained is only limited to the emission sites and other shallow boreholes located at a greater distance from these sites. Lack of geological information from the boreholes, limited groundwater level measurements, lack of aquifer parameters and subsurface geological information within the emission sites are some of the limitations encountered during the project execution. It is therefore important that the scope of work for the Bongwana monitoring project is expanded to allow for more research on the local geology and hydrogeological conditions within the immediate vicinity on either side of the fault. Map the CO_2 migration from the fault into shallow groundwater within the weathered zones. The following work maybe required:

- ERT surveys to map subsurface geological structures around the emission sites,
- Siting and drilling of additional monitoring boreholes to obtain information on local geology along the fault zone,
- Obtain groundwater levels and construct groundwater flow contour maps around emission sites,
- Undertake down-hole EC logging to determine the seepage depth of CO_2,
- Obtain groundwater samples at different depths for hydrochemistry and CO_2 plume monitoring.

This information will allow for better understanding and modelling of the fate and migration of the CO_2 plume within the subsurface geology and obtain insight on the underlying strata and its mineral composition.

REFERENCES

Appelo, C.A.J. and Postma, D. (1994). Geochemistry, groundwater and pollution. 2nd edition, CRC Press, Taylor & Francis Group, London/New York, 648 pp.

Bachu, S (2008). CO_2 storage in geological media: Role, means, status and barriers to deployment. Progress in Energy and Combustion Science, 34, 254–273.

Benson, S.M. (2006). Carbon dioxide capture and storage assessment of Risks from Storage of Carbon Dioxide in Deep Underground Geological Formations. Workshop proceedings, 10-15 solution: Technologies and policies for a Low-Carbon Future. Lawrence Berkeley National laboratory, California, unpublished report, 26 pp.

Benson, S.M, Cook P (2005). Underground geological storage, IPCC special report on carbon dioxide capture and storage, Intergovernmental Panel on Climate, 431pp.

Botha, J.F. (1998). Karoo Aquifers, their geology, geometry and physical properties. WRC Report No: 487/1/98.

British Geological Survey (BGS) (2005). A review of natural CO_2 occurrences and releases and their relevance to CO_2 storage, United Kingdom, 124pp.

Cahill, A.G., Marker, P., and Jakobsen, R. (2014). Hydrogeochemical and mineralogical effects of sustained CO_2 contamination in a shallow sandy aquifer: A field-scale controlled release experiment. Water Resources Research, 50, 1735–1755.

Chabangu, N., Beck, B., Hicks, N., Botha, B., Viljoen, J., Davis, S., and Cloete, M. (2014). The investigation of CO_2 storage potential in the Zululand
Basin in South Africa, South African Center for Carbon Capture and Storage Johannesburg, South Africa, unpublished report, Council for Geoscience, Pretoria, 11pp.

Clayton, C.J., Hay, S.J., Baylis, S.A. and Dipper, B. (1997). Alteration of natural gas during leakage from a North Sea salt diapir field. Marine Geology, Vol.137 (1-2), 69-80.

CO_2GeoNet (2011). Potential impacts on groundwater resources of CO_2 geological storage. IEAGHG, Orchard Business Centre, UK. Report No: 2011/11, 222 pp.

Council for Geoscience. (1988). 1:250 000 Geological Map Series, 2930: Durban, of Southern Africa.

Dafflon, B., Wu, Y., Susan, S.H., Jens, T.B., Thomas, M.D., John, D.P., John, E.P. and Robert, C.T. (2012). Monitoring CO_2 Intrusion and Associated Geochemical Transformations in a Shallow Groundwater System Using Complex Electrical Methods. Environmental science and technology, American chemical society, ACS Publication, 10, 2-8.

D'Amore, F., Panichi, C. (1987). Geochemistry in geothermal exploration. Appl. Geotherm.10, 69-89.

De Decker, R.H. (1981). Geology of the Kokstad area. Explan. Sheet 3028. Department of Minerals and Energy Affairs, Geological Survey, Pretoria, 22pp.

Department of Water and Sanitation (2016). KZN Groundwater Resources information Project (GRIP) borehole database.

Drever, J.I. (1997). The geochemistry of natural waters: surface and groundwater environments. Journal of Environmental Protection, 3rd edition, Prentice Hall, New Jersey, 436pp.

Du Toit, A.L. (1946). The geology of parts of Pondoland, East Griqualand. Explan. Cape sheet 35, Geol. Survey of South Africa, 32pp.

Frye, E., Bao, C., Li, L., and Blumsack, S. (2012) Environmental controls of cadmium desorption during CO_2 leakage. Environmental Science & Technology, 46, 4388–4395.

Gevers, T.W. (1941) Carbon Dioxide springs and exhalations in northern Pondoland and Alfred Country, Natal. Trans. Geol.soc.S.Afr., 38, 233-301.

Grantham, G.H. (1984). The tectonic, metamorphic and intrusive history of the Natal Mobile Belt between Glenmore and Port Edward. M.Sc. Thesis University of Natal, Pietermaritzburg, South Africa, 243pp.

Harris, C., Stock, W.D. and Lanham, J. (1997). Stable Isotopes constraints on the origins of CO_2 gas exhalations at Bongwan, Natal. Department of geological sciences, S.Afri.Geol. 1997.100(3), 261-266.

Hartnady, C.J.H. (1985). Uplifting, seismicity, thermal spring and possible incipient volcanic activity in the Lesotho-Natal region, SE Africa. Tectonics, 4, 371-377.

Harvey, O.R., Qafoku, N.P., Cantrell, K.J., Lee, G., Amonette, J.E., and Brown, C.F., (2012). Geochemical implications of gas leakage associated with geologic CO_2 storage -A qualitative review. Environmental Science & Technology, 47, 23–36.

Ian, C., Tamie, W., Sarah, T., Douglas, A., Michelle, C., Katherine, C. and Joseph, T. (2002). Stable isotope geochemistry of cold CO_2-bearing mineral spring waters, Daylesford, Victoria, Australia: sources of gas and water and links with waning volcanism. Chemical geology 185 (2002) 71-91.

Intergovernmental Panel on Climate Change (IPCC) (2007). Climate Change: impacts, Adaptation and Vulnerability. Working Group II contributing to the 4th assessment report, 976pp.

IPCC (Intergovernmental Panel on Climate Change) (2005). Special Report on Carbon Dioxide Capture and Storage. Prepared by Working Group III of the Intergovernmental Panel on Climate Change, 431pp.

Johnson, G., Hicks, N., Bond, C.E., Gilfillan, S.M.V., Jones, D., Kremer, Y., Lister, R., Nkwane, M., Maupa, T., Munyangane, P., Robey, K., Saunders, I., Pearce, J., Shiton, Z.K and Haszeldine, R.S. (2016). Detection and understanding of natural CO_2 releases in Kwazulu Natal, South Africa. Unpublished paper, 7pp.

Johnson, M.R., Van Vuuren, C.J., Visser, J.N.J., Cole, D.I., Wickens, H., de, V., Christie, A.D.M., Roberts, D.L. (1997). The Foreland Karoo Basin, South Africa. In: Selly, R.C. (Ed.), African Basins. In: Sedimentary Basins of the World, vol. 3. Elsevier Science B.V. Amsterdam, pp. 269–317.

Karolyte, R., Sascha Serno, S.,Johnson, G and Gilfillan, S.M.V. (2017). The influence of oxygen isotope exchange between CO2 and H2O in natural CO2-rich spring waters: Implications for geothermometry. School of GeoSciences, University of Edinburgh, Grant Institute, James Hutton Road, Edinburgh, EH9 3FE, United Kingdom, 15pp.

Kharaka, Y.K. (2009). Changes in the chemistry of shallow groundwater related to the 2008 injection of CO_2 at the ZERT field site, Bozeman, Montana, 47pp.

Kharaka, Y.K., Thordsen, J.J., Kakouros, E., Ambats, G., Herkelrath, W.N., Beers, S.R., Birkholzer, J.T., Apps, J.A., Spycher, N.F., and Zheng, L. (2010). Changes in the chemistry of shallow groundwater related to the 2008 injection of CO_2 at the ZERT field site, Bozeman, Montana. Environmental Earth Sciences, 60, 273–284.

King G. (1998). 1:500 000 Hydrogeological Map series of South Africa, 2930 Durban.

Kingsley, C.S. (1975). A new stratigraphic classification implying a lithofacies change in the Table Mountain Sandstone in southern Natal. Transactions and Proceedings of the Geological Society of South Africa, 78, 43–55.

Lemieux, J.M. (2011) Review: The potential impact of underground geological storage of carbon dioxide in deep saline aquifers on shallow groundwater resources. Hydrogeology Journal, 19, 757–778.

Little, M.G. and Jackson, R.B. (2010). Potential impacts of leakage from deep CO_2 geosequestration on overlying freshwater aquifers. Environmental Science & Technology, 44, 9225–9232.

Liu, F., Song, X., Yang, L., Zhang, Y., Han, D., Ma, Y and Bu, H (2015). Identifying the origin and geochemical evolution of groundwater using hydrochemistry and stable isotopes in the Subei Lake basin, Ordos energy base, Northwestern China, Hydrol.Earth Syst.Sci., 19, 551-565.

Lu, J., Partin, J.W., Hovorka, S.D., and Wong, C. (2010). Potential risks to freshwater resources as a result of leakage from CO_2 geological storage: a batch-reaction experiment. Environmental Earth Sciences, 60, 335–348.

MacCourt, S., Amstrong, R.A., Grantham, G.H. and Thomas, R.J. (2006). Geology and evolution of the Natal belt, South Africa. Elsevier, Journal of African Earth Science 46 (2006), 71-92.

Marghade, D., Malpe, D. B., and Zade, A. B. (2012). Major ion chemistry of shallow groundwater of a fast growing city of Central India, Environ. Monit. Assess. 184, 2405–2418. https://doi.org/10.1007/s10661.

Marshall, C.G.A. (1999). The stratigraphy and origin of the Msikaba formation. *South African Journal of Geology,* 102, 15–25.

Mendonidis, P., Grantham, G.H. (2003). Petrology, origin and metamorphic history of proterozoic-aged granulites of the Natal Metamorphic Province, Southeastern Africa. Gondwana Research 6, 607–628.

Naseem, S., Rafique, T., Bashir, E., Bhanger, M. I., Laghari,A., and Usmani, T. H. (2010) Lithological influences on occurrence of high-fluoride groundwater in Nagar Parkar area, Thar Desert, Pakistan, Chemosphere, 78, 1313–1321. https://doi.org/10.1016/j.chemosphere.2010.01.010.

Newmark, R.L., Friedmann, S.J., and Carroll, S.A., (2010), Water challenges for geologic carbon capture and sequestration. Environmental Management, 45, 651–661.

Otto, J.D.T. (1977). The geology and petrology of the Marble Delta. Annale Univ. Stellenbosch., Ser. AI-(geol) 2, 249–365.

Parkhurst, D.L., and Appelo, C.A.J. (1999). User's guide to PHREEQC (Version 2), A computer program for speciation, batch-reaction, one-dimensional transport, and inverse geochemical calculations: U.S. Geological Survey Water-Resources Investigations Report 99–4259, 312 pp.

Parsons, R. (1995). A South African aquifer system management classification. Department of Water Affairs and Forestry, Stellenbosch, WRC report No.KV77/95.

Piper, A. M. (1953) A graphic procedure in the geochemical interpretation of water analysis, US Department of the Interior, Geological Survey, Water Resources Division, Groundwater Branch, Washington, 63pp.

Plummer, L. N. (1992) Geochemical Modeling of Water-Rock Interaction: Past, Present, Future," in Water-Rock Interation, Vol. 1, Kharaka, Y. K. & Maest, A. S. (Eds.), Balkema, Rotterdam, Brookfield, 858 pp.

SACS, (1980). Stratigraphy of South Africa. Geological Survey of South Africa, Handbook 8, 690pp.

Shipton, Z.K., and Haszeldine, R.S. (2016). Detection and understanding of natural CO_2 releases in KwaZulu-Natal, South Africa, unpublished report, Council for Geosciences, 56pp.

Siirila, E.R., Navarre-Sitchler, A.K., Maxwell, R.M., and McCray, J.E., (2012), A quantitative methodology to assess the risks to human health from CO_2 leakage into groundwater. Advances in Water Resources, 36, 146–164.

Smyth, J.M., (2008). Assessing risk to fresh water resources from long term CO_2 injection- laboratory and field studies: presented at the 9th International Conference on Greenhouse Gas Control Technologies (GHGT-9), Washington, D.C. GCCC Digital Publication Series #08-03j.

Snoeyink V. and Jenkins. D. (1980). Water Chemistry. JOHN WILEY & SONS, New York, 382pp.

Terzi, K., Aggelopoulos, C.A., Bountas, I., and Tsakiroglou, C.D. (2014). Effects of carbon dioxide on the mobilization of metals from Aquifers. Environmental Science & Technology, 48, 4386–4394.

Thomas, R.J. (1988). The geology of the Portshepstone Area. Explan. sheet 3030. Dept. Miner. Energy Affairs, Geological Survey of South Africa, 32pp.

Torres, R.L., GARCÍA, A., and GARCÍA, P.A., (2000). An integrated workplace for the graphical and algebraic analysis of phase assemblages on 32-bit Wintel platforms. Computers and Geosciences 26, 779-793. https://doi.org/10.1016/S0098-3004(00)00006-6.

Von Brunn, V. (1994). Glaciogenic deposits of the Permo-Carboniferous Dwyka Group in the eastern region of the Karoo Basin, South Africa, in Deynoux, M., Miller, J.M.G., Domack, E.W., Eyles, N., Fairchild, I.J., and Young, G.M., eds., Earth's Glacial Record: Cambridge, Cambridge University Press, 60–69.

Wang, S and Jaffe, P.R. (2004). Dissolution of a mineral phase in potable aquifers due to CO2 releases from deep formations; effect of dissolution kinetics. Energy Convers Manage 45:2833–2848.

Weaver,J.M.C., Lisa, C. and Siep Talma, A. (2007). Groundwater sampling: a comprehensive guide for groundwater sampling prepared for the Water Research Commission. Republic of South Africa. ISBN 978-1-77005-545-2 Set 1-874858-46-2.

Wilkin, R. T., and D. C. Digiulio. (2010). Geochemical Impacts to Groundwater from Geologic Carbon Sequestration: Controls on pH and Inorganic Carbon Concentrations from Reaction Path and Kinetic Modeling. *Environmental Science & Technology* no. 44 (12):4821-4827. https://doi.org/10.1021/es100559j.

WRC (Water research Commission) (2002). Hydrogeology of the main Karoo Basin. Report NoTT179/02.

Xing, L., Guo, H., and Zhan, Y. (2013). Groundwater hydrochemical characteristics and processes along flow paths in the North China Plain, J. Asian Earth Sci., 70–71, 250–264,doi:10.1016/j.jseaes.2013.03.017.

Yang, C.; Delgado-Alonsob, J.; Susan, H.; Patrick, M., Ramon, T. and Straun, P. (2014). Monitoring dissolved CO_2 in groundwater for CO_2 leakage detection in a shallow aquifer. Bureau of Economic Geology, The University of Texas at Austin, 10100 Burnet Rd., Austin, TX, 78758 USA, 8pp.

Yang, L., Song, X., Zhang, Y., Yuan, R., Ma, Y., Han, D., and Bu, H. (2012) A hydrochemical framework and water quality assessment of river water in the upper reaches of the Huai River Basin, China, Environ. Earth Sci., 67, 2141–2153, doi: 10.1007/s12665- 012-1654-7.

Young, M.A. (1923). Exhalations of carbon dioxide in Alfred Country, Natal. Geological Society of Southern Africa, 99-102.

Zheng, L., Apps, J., Spycher, N., Birkholzer, J., Kharaka, Y.K., Thordsen, J., Kakouros, E., Trautz, R., Rauch, H. and Gullickson, K. (2009). Changes in shallow groundwater chemistry at the 2008 ZERT CO_2 injection experiment: II-modeling analysis. Abstract, eight carbon capture and sequestration conference, Pittsburgh, 36pp.

APPENDIX A: BOREHOLE INFORMATION FOR THE GRIP DATA BASE OF THE STUDY AREA (DW&S, 2016)

Table 8-1: GRIP boreholes (Hydrochemistry and water levels)

Site ID	Latitude	Longitude	WL (mbgl)	WL Elevation (mamsl)	Altitude mamsl)	pH	EC(mS/m)	TDS (mg/l)	Ca (mg/l)	HCO3 (mg/l)	MALK (mg/l)	PALK (mg/l)	Na(mg/l)	Mg (mg/l)	Mn (mg/l)	Al (mg/l)	CO3 (mg/l)	Fe (mg/l)	SO4 (mg/l)	Cl (mg/l)	N (mg/l)	Si (mg/l)	K (mg/l)
3030BAK0044	-30.68936	30.03255	51.78	488.22	540	6.9	14	1	2.3	1	1	1	18	3.2	0.04	1	1	0.12	2.6	16	1.83	1	1.9
3029DD0010	-30.815333	29.988878	55.56	623.44	679	7.7	90.9	671	60.4	-	-	-	83.9	37.9	-	-	-	-	-	-	-	-	2.1
3029DB00048	-30.747296	29.960727	98.00	627.00	725	-	-	-	-	-	-	-	-	-	-	-	-	-	-	-	-	-	-
3029DB00039	-30.73057	29.965487	85.00	664.00	749	8.3	55.3	408	21.8	-	-	-	57.3	20.3	-	-	-	-	-	-	-	2.5	9.4
3029DBR0002	-30.727609	29.996314	23.10	736.90	760	7	55	357	34	1	1	1	30	18	20	1	1	180	2.36	38	6.81	1	0.7
3029DB00041	-30.731287	29.992759	10.00	731.00	741	8.16	27.5	211	15	-	103	1	25.2	8.2	-	-	-	-	-	-	-	14.8	5.1
3029DB00019	-30.729298	29.988938	16.00	742.00	758	7.75	11	89	8.7	-	-	-	6.2	4	-	-	-	-	-	-	-	16.5	0.3
3030CC00075	-30.781095	30.007652	33.00	642.00	675	8.1	53	-	-	-	-	-	-	-	-	-	-	-	-	-	-	-	-
3030CA00107	-30.745797	30.030793	52.00	644.00	696	8.1	39	-	-	-	-	-	-	-	-	-	-	-	-	-	-	-	-
3029DD00016	-30.769945	29.993739	48.00	647.00	695	7.97	50.6	400	33.6	-	-	-	37.9	24.6	-	-	-	-	-	-	-	8.6	6.4
3029DD00024	-30.779495	29.993419	15.00	645.00	660	-	-	-	-	-	-	-	-	-	-	-	-	-	-	-	-	-	-
3029DD00014	-30.804674	29.998779	55.00	659.00	714	7.44	34.9	262	11.4	-	-	-	47.8	5.8	-	-	-	-	-	-	-	10.4	7.2
3029DB00061	-30.694099	29.924525	18.00	798.00	816	7.6	15	-	-	-	-	-	-	-	-	-	-	-	-	-	-	-	-
3029DB00018	-30.735997	29.998929	35	709	744	7.4	48	-	-	-	-	-	-	-	-	-	-	-	-	-	-	-	-
3030CA00108	-30.737627	30.000502	93	661	754	-	-	-	-	-	-	-	-	-	-	-	-	-	-	-	-	-	-
3030CA00109	-30.742627	30.004842	33	705	738	8	44	-	-	-	-	-	-	-	-	-	-	-	-	-	-	-	-
3030CA00110	-30.739297	30.011982	46	665	711	7.9	59	-	-	-	-	-	-	-	-	-	-	-	-	-	-	-	-
3030CA00101	-30.743247	30.009842	85	639	724	7.91	76.8	583	46.6	-	-	-	75.1	27.9	-	-	-	-	-	-	-	7.1	3
3030CC00076	-30.761596	30.005452	18	658	676	7.9	22	-	-	-	-	-	-	-	-	-	-	-	-	-	-	-	-
3029DD00017	-30.754776	29.994499	54	660	714	8.13	38.6	323	19.3	-	-	-	41	13.7	-	-	-	-	-	-	-	5.6	8.9
3029DD00015	-30.769055	29.996979	25	652	677	7.37	49.3	364	28.3	-	-	-	42	20.1	-	-	-	-	-	-	-	11.8	3.2
3029DD00026	-30.776295	29.992258	31	624	655	7.6	48	-	-	-	-	-	-	-	-	-	-	-	-	-	-	-	-
3029DD00021	-30.812793	29.993078	15	647	662	-	-	-	-	-	-	-	-	-	-	-	-	-	-	-	-	-	-
3029DD00013	-30.821873	29.987618	20	630	650	7.57	70.7	533	47.3	-	-	-	63.1	29.2	-	-	-	-	-	-	-	7.6	2.7

APPENDIX B: TRACE ELEMENT COMPOSITION FOR GROUNDWATER AND SURFACE WATER SITES

Sample ID		BGN-1	BGN-2	BGN-3	BGN-4	BGN-6	BGN-7	BGN-8	BGN-9	BGN-11	BGN-12	BGN-14	BGN-15	BGN-16	BGN-17	BGN-20	BGN-21	BGN-22
Element	**Units**																	
Li	**ug/l**	**4.767**	**4.767**	**4.767**	**9.534**	**4.767**	**4.767**	**9.534**	4.767	38.137	47.671	4.767	57.205	57.205	4.767	9.534	4.767	4.767
Be	**ug/l**	2.006	2.006	2.006	4.013	2.006	4.013	2.006	2.006	16.051	20.064	2.006	24.077	24.077	2.006	4.013	2.006	2.006
B	**ug/l**	18.12	36.25	54.38	36.25	36.25	12.687	6.344	18.12	580.01	362.01	54.38	217.5	652.5	36.25	12.687	6.344	6.345
Al	**ug/l**	14.69	22.04	2.45	1.714	0.000857	4.9	7.35	2.45	117.54	342.84	31.84	352.63	117.54	7.35	1.714	9.79	9.79
Si	**mg/l**	1.82	1.77	6.29	2.12	3.3	3.16	3.66	1.2	2.59	2.05	1.47	1.86	2.12	2.62	3.27	3.67	2.53
S	**mg/l**	1.99	0.3983	1.99	2.39	3.98	3.19	0.3983	1.59	31.86	11.95	1.19	28.68	62.13	1.59	0.7965	0.7965	2.79
Sc	**ug/l**	16.17	9.49	10.72	21.09	11.07	27.42	12.48	11.6	89.98	105.45	11.6	105.44	115.99	11.07	23.55	11.25	11.6
Ti	**(ng/l)**	585.352	585.352	585.352	0.000117	585.352	0.000117	585.352	585.352	0.000468	0.000585	585.352	0.000702	0.000702	585.352	0.000117	585.352	585.352
V	**(ng/l)**	726.37	598.18	4830	85.45	726.37	427.25	1750	14.953	119.628	854.49	897.3	512.69	1030	384.54	85.45	42.72	469.99
Cr	**(ng/l)**	363.05	332.79	3810	363.04	423.56	242.02	121.01	302.54	2420	2720	363.05	3270	3630	181.52	363.04	151.26	211.77
Co	**(ng/l)**	31.63	31.36	5.487	156.79	47.04	62.71	47.04	47.04	43.899	54.874	156.79	65.849	65.849	5.487	564.47	47.04	5.487
Ni	**(ng/l)**	616.09	1030	924.16	821.44	975.51	308.03	513.04	1750	3290	179.683	667.44	10470	3080	102.68	1130	513.4	667.44
Cu	**(ng/l)**	1090	1040	520.31	466.44	233.22	968.84	304.99	304.99	717.58	62.787	412.64	430.54	430.54	161.46	394.68	233.22	287.05
Zn	**(ug/l)**	17.67	10.73	10.89	477.62	441.17	1370	208.54	123.39	3.96	6.6	3.47	9.9	5.94	4.13	11.22	5.94	240.65
Ga	**(ug/l)**	5.57	4.18	9.45	2.39	2.49	3.18	2.39	1.59	0.2785	0.3481	0.6961	4.77	2.39	2.19	5.17	2.88	0.9946
Ge	**(ng/l)**	67.592	67.592	67.592	386.24	67.592	135.184	67.592	67.592	1540	1930	67.592	811.104	811.104	67.592	135.184	67.592	67.592
As	**(ng/l)**	97.199	277.71	555.43	194.397	97.199	194.397	97.199	555.43	777.59	971.987	277.71	11660	3330	833.14	555.42	277.71	277.71
Se	**(ug/l)**	1.832	5.23	1.832	3.663	1.832	3.663	1.832	1.832	14.653	18.317	1.832	21.98	21.98	1.832	3.663	1.832	1.832
Br	**(ug/l)**	39.33	52.44	65.55	305.91	52.44	139.83	34.96	21.85	559.32	436.96	13.11	471.91	576.79	78.66	262.2	48.07	26.22
Rb	**(ng/l)**	341.31	227.54	39.819	2280	113.77	682.62	455.08	39.819	40060	47790	1480	79210	36870	39.819	455.08	227.54	227.54
Sr	**(ug/l)**	20.69	18.63	31.01	149.5	55.1	47.84	22.13	32.18	417.07	433.19	12.27	466.98	485.31	15.76	76.75	30.2	83.96
y	**(ug/l)**	12.24	11.63	11.24	22.67	11.66	23.71	10.56	10.36	94.06	115.63	10.01	140.7	151.61	10.88	21.7	10.82	11.11
Zr	**(ng/l)**	27.75	9.712	55.5	55.5	27.75	111	9.712	9.712	1110	3890	9.712	2660	4660	55.5	222	9.712	27.75
Nb	**(ng/l)**	4.063	4.063	4.063	8.125	4.063	8.125	4.063	4.063	32.501	40.626	4.063	48.751	48.751	4.063	8.125	4.063	4.063
Mo	**(ng/l)**	15.513	15.513	1323.97	88.64	221.61	177.29	44.32	576.22	124.101	155.1261	15.513	186.151	186.151	15.513	31.025	15.513	44.32
Ru	**(ng/l)**	9.098	9.098	9.098	18.196	9.098	18.196	9.098	9.098	72.785	90.981	9.098	109.177	109.177	9.098	18.196	9.098	9.098
Rh	**(ng/l)**	1.556	1.556	1.556	3.112	1.556	3.112	1.556	1.556	12.447	15.559	1.556	18.671	18.671	1.556	3.112	1.556	1.556
Pd	**(ng/l)**	7.36	7.36	7.36	14.719	7.36	14.719	7.36	7.36	58.877	73.597	7.36	88.316	88.316	7.36	14.719	7.36	7.36
Ag	**(ng/l)**	13.47	13.47	26.94	9.43	13.47	9.43	4.715	13.47	37.718	47.148	4.715	56.577	56.577	4.715	26.94	13.47	26.94
Cd	**(ng/l)**	38.579	38.579	110.23	77.158	38.579	77.158	38.579	38.579	308.632	385.79	38.579	462.948	462.948	38.579	77.158	38.579	38.579
In	**(ug/l)**	9.25	9.11	9.02	15.86	9	15.9	8.96	7.75	61.46	74.6	8.33	91.39	84.17	8.55	15.81	7.93	7.62
Sn	**(ng/l)**	21.737	21.737	21.737	124.21	124.21	43.475	21.737	21.737	173.899	217.374	21.737	260.849	260.849	21.737	43.475	21.737	21.737
Sb	**(ng/l)**	238.38	524.44	286.05	286.05	238.38	190.7	238.38	47067	381.39	166.859	143.02	572.09	200.231	190.7	190.7	95.35	190.7
Te	**(ng/l)**	813.151	813.151	813.151	1626	813.151	1626	813.151	813.151	6505	8132	813.151	9758	9758	813.151	1626	813.151	813.151
I	**(ug/l)**	2.26	4.52	2.26	9.69	2.26	12.27	2.58	0.6457	5.17	16.14	1.29	7.75	27.12	3.55	11.62	3.55	0.9685
Cs	**(ng/l)**	11.643	11.643	11.643	23.287	33.27	199.6	11.643	33.27	4260	8980	232.87	5190	8380	11.643	23.287	99.8	166.34
Ba	**(ug/l)**	36.61	29.68	65.43	13.83	15.99	12.29	12.14	9.53	12.29	7.68	3.53	11.06	14.75	14.45	32.59	22.91	10.45
La	**(ng/l)**	51.02	3.571	3.571	7.143	3.571	7.143	3.571	20.41	28.571	35.714	71.43	42.856	42.856	3.571	7.143	3.571	3.571
Ce	**(ng/l)**	31.52	7.88	23.64	15.76	15.76	5.515	7.88	7.88	22.061	27.576	165.47	33.091	33.091	2.758	5.515	15.76	2.758
Pr	**(ng/l)**	8.69	3.043	3.043	6.086	3.043	6.086	3.043	3.043	24.344	30.43	8.69	36.516	36.516	3.043	6.086	3.043	3.043
Nd	**(ng/l)**	15.593	15.593	15.593	31.185	15.593	31.185	15.593	44.55	124.741	155.927	44.55	187.112	187.112	15.593	89.1	15.593	15.593
Sm	**(ng/l)**	18.434	52.67	18.434	36.869	18.434	36.869	18.434	18.434	147.474	184.343	18.434	221.212	221.212	18.434	36.869	18.434	18.434
Eu	**(ng/l)**	4.591	4.591	4.591	9.181	4.591	9.181	4.591	4.591	36.724	45.905	4.591	55.086	55.086	4.591	9.181	4.591	4.591
Gd	**(ng/l)**	8.923	8.923	8.923	17.845	8.923	17.845	8.923	8.923	71.381	254.93	25.49	107.071	107.071	8.923	17.845	8.923	8.923
Tb	**(ug/l)**	7.5	7.18	6.52	12.44	7.12	13.92	6.8	6.75	50.9	64.85	6.22	77	72.68	5.71	12.62	5.8	6.13
Dy	**(ng/l)**	7.323	7.323	7.323	14.646	7.323	14.646	7.323	7.323	58.583	418.45	7.323	87.874	87.874	7.323	147.646	7.323	7.323
Ho	**(ng/l)**	1.677	1.677	1.677	3.354	1.677	3.354	1.677	1.677	13.415	47.91	1.677	20.122	20.122	1.677	9.58	1.677	1.677
Er	**(ng/l)**	4.933	4.933	4.933	9.866	4.933	9.866	4.933	4.933	39.462	281.88	14.09	59.193	59.193	4.933	9.866	4.933	4.933
Tm	**(ng/l)**	1.48	1.48	1.48	2.96	1.48	2.96	1.48	1.48	11.839	14.799	1.48	17.759	17.759	1.48	2.96	1.48	1.48

Sample ID		BGN-1	BGN-2	BGN-3	BGN-4	BGN-6	BGN-7	BGN-8	BGN-9	BGN-11	BGN-12	BGN-14	BGN-15	BGN-16	BGN-17	BGN-20	BGN-21	BGN-22
Element	**Units**																	
Yb	**(ng/l)**	6.443	18.41	6.443	12.885	18.41	12.885	6.443	6.443	51.541	64.427	6.443	220.89	77.312	6.443	12.885	6.443	6.443
Lu	**(ng/l)**	3.058	8.74	8.74	34.95	26.21	34.95	17.47	43.69	69.89	436.85	8.74	104.84	209.69	8.74	17.47	17.47	26.21
Hf	**(ng/l)**	5.16	5.16	5.16	10.319	5.16	10.319	5.16	5.16	41.278	51.597	5.16	61.916	61.916	5.16	10.319	5.16	5.16

APPENDIX C: TRACE ELEMENT COMPOSITION OF THE TRAVERTINE CONE

Sample Name	Sc	V	Cr	Co	Ni	Cu	Zn	Ga	Ge	As	Se	Rb	Sr	Y	Zr	Nb	Mo	Cd	In	Sn	Sb	Te	U
ML3	2.65	22.84	72.28	10.06	25.16	18.41	13.50	2.25	2.09	1.15	< 1.6	13.75	613.11	4.10	56.20	4.83	0.58	< 0.46	< 0.03	1.24	1.18	< 0.86	0.61
ML4	0.40	4.36	8.97	0.75	5.62	13.27	4.28	0.16	1.62	0.60	< 1.6	1.37	652.73	0.40	3.18	1.38	0.45	< 0.46	0.04	0.60	1.24	< 0.86	0.24

Sample Name	Cs	Ba	La	Ce	Pr	Nd	Sm	Eu	Gd	Tb	Dy	Ho	Er	Tm	Yb	Lu	Hf	Ta	W	Tl	Pb	Bi	Th
ML3	4.66	110.18	3.71	8.67	0.82	3.31	0.60	0.14	0.65	0.10	0.59	0.14	0.46	0.08	0.50	0.04	1.43	0.10	0.26	< 0.06	2.16	< 0.08	1.41
ML4	0.69	71.22	0.27	0.53	0.08	0.27	< 0.15	< 0.06	0.12	< 0.02	0.09	0.03	< 0.06	< 0.02	< 0.1	< 0.04	0.06	0.02	0.14	< 0.06	0.31	< 0.08	0.09